

AD-A023 356

A WIND TUNNEL STUDY OF THE EFFECTS OF TRAILING EDGE
MODIFICATIONS ON THE LIFT-DRAG RATIO OF A CIRCULATION
CONTROLLED AIRFOIL

Vayl S. Oxford

Air Force Institute of Technology
Wright-Patterson Air Force Base, Ohio

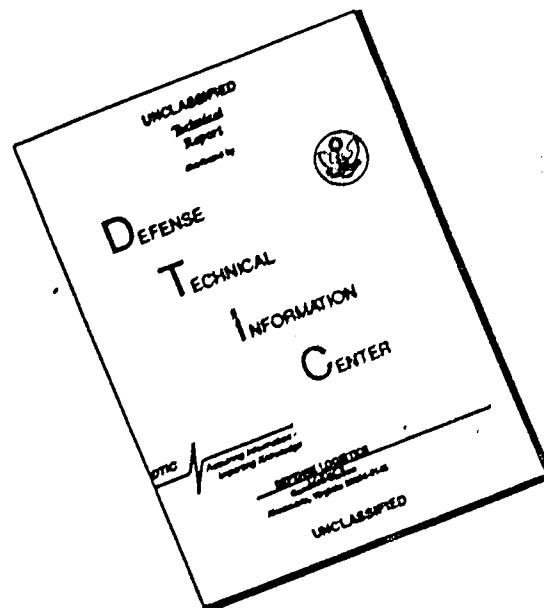
December 1975

DISTRIBUTED BY:

NTIS

National Technical Information Service
U. S. DEPARTMENT OF COMMERCE

DISCLAIMER NOTICE



THIS DOCUMENT IS BEST QUALITY AVAILABLE. THE COPY FURNISHED TO DTIC CONTAINED A SIGNIFICANT NUMBER OF PAGES WHICH DO NOT REPRODUCE LEGIBLY.

KEEP UP TO DATE

Between the time you ordered this report—which is only one of the hundreds of thousands in the NTIS information collection available to you—and the time you are reading this message, several *new* reports relevant to your interests probably have entered the collection.

Subscribe to the **Weekly Government Abstracts** series that will bring you summaries of new reports as soon as they are received by NTIS from the originators of the research. The WGA's are an NTIS weekly newsletter service covering the most recent research findings in 25 areas of industrial, technological, and sociological interest—invaluable information for executives and professionals who must keep up to date.

The executive and professional information service provided by NTIS in the **Weekly Government Abstracts** newsletters will give you thorough and comprehensive coverage of government-conducted or sponsored re-

search activities. And you'll get this important information within two weeks of the time it's released by originating agencies.

WGA newsletters are computer produced and electronically photocomposed to slash the time gap between the release of a report and its availability. You can learn about technical innovations immediately—and use them in the most meaningful and productive ways possible for your organization. Please request NTIS-PR-205/PCW for more information.

The weekly newsletter series will keep you current. But *learn what you have missed in the past* by ordering a computer **NTISearch** of all the research reports in your area of interest, dating as far back as 1964, if you wish. Please request NTIS-PR-186/PCN for more information.

WRITE: Managing Editor
5285 Port Royal Road
Springfield, VA 22161

Keep Up To Date With SRIM

SRIM (Selected Research in Microfiche) provides you with regular, automatic distribution of the complete texts of NTIS research reports *only* in the subject areas you select. SRIM covers almost all Government research reports by subject area and/or the originating Federal or local government agency. You may subscribe by any category or subcategory of our WGA (**Weekly Government Abstracts**) or **Government Reports Announcements and Index** categories, or to the reports issued by a particular agency such as the Department of Defense, Federal Energy Administration, or Environmental Protection Agency. Other options that will give you greater selectivity are available on request.

The cost of SRIM service is only 45¢ domestic (60¢ foreign) for each complete

microfiched report. Your SRIM service begins as soon as your order is received and processed and you will receive biweekly shipments thereafter. If you wish, your service will be backdated to furnish you microfiche of reports issued earlier.

Because of contractual arrangements with several Special Technology Groups, not all NTIS reports are distributed in the SRIM program. You will receive a notice in your microfiche shipments identifying the exceptionally priced reports not available through SRIM.

A deposit account with NTIS is required before this service can be initiated. If you have specific questions concerning this service, please call (703) 451-1558, or write NTIS, attention SRIM Product Manager.

This information product distributed by

NTIS

U.S. DEPARTMENT OF COMMERCE
National Technical Information Service
5285 Port Royal Road
Springfield, Virginia 22161

REPORT DOCUMENTATION PAGE		READ INSTRUCTIONS BEFORE COMPLETING FORM
1. REPORT NUMBER GAE/AE/75D-16	2. GOVT ACCESSION NO.	3. RECIPIENT'S CATALOG NUMBER AD A023356
4. TITLE (and Subtitle) A WIND TUNNEL STUDY OF THE EFFECTS OF TRAILING EDGE MODIFICATIONS ON THE LIFT-DRAG RATIO OF A CIRCULATION CONTROLLED AIRFOIL		5. TYPE OF REPORT & PERIOD COVERED MS Thesis
7. AUTHOR(s) Vayl S. Oxford 2Lt USAF		6. PERFORMING ORG. REPORT NUMBER
9. PERFORMING ORGANIZATION NAME AND ADDRESS Air Force Institute of Technology (AFIT/EN) Wright-Patterson AFB, Ohio 45433		8. CONTRACT OR GRANT NUMBER(s)
11. CONTROLLING OFFICE NAME AND ADDRESS Aeronautical Systems Division (ASD/XRHD) Wright-Patterson AFB, Ohio 45433		10. PROGRAM ELEMENT, PROJECT, TASK AREA & WORK UNIT NUMBERS
14. MONITORING AGENCY NAME & ADDRESS (if different from Controlling Office)		12. REPORT DATE December, 1975
		13. NUMBER OF PAGES 68
		15. SECURITY CLASS. (of this report) Unclassified
		15a. DECLASSIFICATION DOWNGRADING SCHEDULE
16. DISTRIBUTION STATEMENT (of this Report) Approved for public release; distribution unlimited.		
17. DISTRIBUTION STATEMENT (of the abstract entered in Block 20, if different from Report) IS SUBJECT TO		
18. SUPPLEMENTARY NOTES Approved for public release; IAW 190-17 Jerry C. Hix, Captain, USAF		
19. KEY WORDS (Continue on reverse side if necessary and identify by block number) Airfoil Testing Boundary Layer Control Blowing Circulation Control Trailing Edge Contours REPRODUCED BY NATIONAL TECHNICAL INFORMATION SERVICE U. S. DEPARTMENT OF COMMERCE SPRINGFIELD, VA. 22161		
20. ABSTRACT (Continue on reverse side if necessary and identify by block number) Wind tunnel tests were conducted to determine the effects of trailing edge modifications on the lift-to-drag ratio of a circulation controlled airfoil. The model was a 20 percent thick, five percent cambered, elliptical airfoil. The airfoil was modified in aft contour, blowing slot position, and blowing angle. A 1.5 inch splitter plate was mounted at the 99 percent chord for all tests. The tests were run at a Reynolds Number, based on model chord, of 7.41×10^5 , while the angle of attack and blowing rate were varied during each test sequence.		

UNCLASSIFIED

SECURITY CLASSIFICATION OF THIS PAGE(When Data Entered)

Block 20. (Continued)

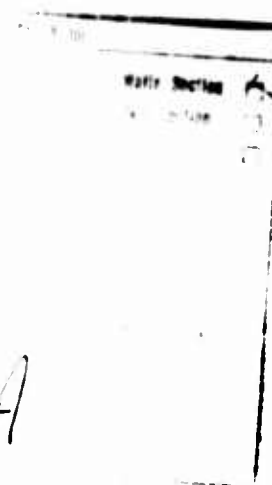
It was found that the modifications caused increases in the section lift coefficient and decreases in the section total drag coefficients as compared to the original airfoil. Due to these results, the lift-to-drag ratio for airfoils using modifications were higher than the original airfoil. A comparison of the results for these modified airfoils revealed that there were no drastic differences due to the modifications. This indicated that the changes made provided for little variation in results, and that such changes needed to be of greater magnitude.

1 a

UNCLASSIFIED

SECURITY CLASSIFICATION OF THIS PAGE(When Data Entered)

GAE/AE/75D-16



A

A WIND TUNNEL STUDY OF THE EFFECTS
OF TRAILING EDGE MODIFICATIONS ON
THE LIFT-DRAG RATIO OF A
CIRCULATION CONTROLLED AIRFOIL

THESIS

GAE/AE/75D-16

Vayl S. Oxford
2d Lt USAF

Approved for public release; distribution unlimited.



A

A WIND TUNNEL STUDY OF THE EFFECTS OF
TRAILING EDGE MODIFICATIONS ON THE
LIFT-DRAG RATIO OF A CIRCULATION
CONTROLLED AIRFOIL

THESIS

Presented to the Faculty of the School of Engineering
of the Air Force Institute of Technology

Air University

in Partial Fulfillment of the
Requirements for the Degree of
Master of Science

by

Vayl S. Oxford, B.S.

2d Lt

USAF

Graduate Aeronautical Engineering

December 1975

Approved for public release; distribution unlimited.

1-0

Preface

This study investigated the effects of trailing edge modifications on the lift-to-drag ratio of a cambered, elliptical, circulation controlled airfoil. It is hoped that the results will be of value in the optimization of such high lift airfoils.

I would like to express my appreciation to Dr. Milton E. Franke, my advisor, Professor Harold C. Larsen, and Mr. James Snyder ASD/XRH, for their assistance throughout the study. In addition, I would like to express my appreciation to Mr. Millard Wolfe and the AFIT workshop staff for their work on the airfoil modifications. Further gratitude is expressed to Mr. Wales S. Whitt for his advice and assistance during the wind tunnel operation.

Mr. Julius Becsey, AFAPL, deserves many thanks for his help with the data reduction program and for the use of his equipment. Additional thanks go to Mr. George Lorraine and the Tech Photo staff for their photographic support.

Vayl S. Oxford

Contents

	Page
Preface	ii
List of Figures	v
List of Tables	vi
List of Symbols	vii
Abstract	viii
I. Introduction	1
Previous Studies	1
Present Study	2
Scope	3
II. Description of Apparatus	4
Wind Tunnel	4
Airfoil	4
Airfoil Modifications	5
Pitot Tube Apparatus	6
Flowmeter	7
Oil Filter	7
Wake Survey Rake	8
Manometers	8
III. Experimental Procedures	9
IV. Data Reduction	11
Section Lift Coefficient	11
Momentum Coefficient	11
Section Total Drag Coefficient	12
Lift-to-Drag Ratio	13
Wind Tunnel Corrections	14

Contents

	Page
V. Results and Discussion	15
General Observations	15
Lift Results	16
Drag Results	19
Lift-to-Drag Results	20
VI. Conclusions	22
VII. Recommendations	23
Bibliography	24
Appendix A: Apparatus	25
Appendix B: Data	31
Vita	55

List of Figures

<u>Figure</u>		<u>Page</u>
1	Cross Section of the Airfoil With Endpiece Attached	26
2	Trailing Edge Configurations 1-B and 2-B	27
3	Trailing Edge Configurations 3-B and 5-B	28
4	Oil Filtering System	29
5	The Effect of C_μ on C_l for Eight Airfoil Configurations at -6 Degrees Angle of Attack	32
6	The Effect of C_μ on C_l for Eight Airfoil Configurations at -4 Degrees Angle of Attack	33
7	The Effect of C_μ on C_l for Eight Airfoil Configurations at -2 Degrees Angle of Attack	34
8	The Effect of C_μ on C_l for Eight Airfoil Configurations at 0 Degrees Angle of Attack	35
9	The Effect of C_μ on C_l for Eight Airfoil Configurations at +2 Degrees Angle of Attack	36
10	The Effect of C_μ on C_l for Eight Airfoil Configurations at +4 Degrees Angle of Attack	37
11	The Effect of C_μ on C_l for Eight Airfoil Configurations at +6 Degrees Angle of Attack	38
12	The Effect of C_μ on C_{d_t} for Eight Airfoil Configurations at -6 Degrees Angle of Attack	39
13	The Effect of C_μ on C_{d_t} for Eight Airfoil Configurations at -4 Degrees Angle of Attack	40
14	The Effect of C_μ on C_{d_t} for Eight Airfoil Configurations at -2 Degrees Angle of Attack	41
15	The Effect of C_μ on C_{d_t} for Eight Airfoil Configurations at 0 Degrees Angle of Attack	42

List of Figures

<u>Figure</u>		<u>Page</u>
16	The Effect of C_{μ} on C_{d_t} for Eight Airfoil Configurations at +2 Degrees Angle of Attack	43
17	The Effect of C_{μ} on C_{d_t} for Eight Airfoil Configurations at +4 Degrees Angle of Attack	44
18	The Effect of C_{μ} on C_{d_t} for Eight Airfoil Configurations at +6 Degrees Angle of Attack	45
19	The Effect of C_{μ} on C_{d_o} and C_{d_t} at 0 Degrees Angle of Attack	46
20	The Effect of C_{μ} on C_{d_o} and C_{d_t} at 0 Degrees Angle of Attack	47
21	The Effect of C_{μ} on l/d for Eight Airfoil Configurations at -6 Degrees Angle of Attack	48
22	The Effect of C_{μ} on l/d for Eight Airfoil Configurations at -4 Degrees Angle of Attack	49
23	The Effect of C_{μ} on l/d for Eight Airfoil Configurations at -2 Degrees Angle of Attack	50
24	The Effect of C_{μ} on l/d for Eight Airfoil Configurations at 0 Degrees Angle of Attack.	51
25	The Effect of C_{μ} on l/d for Eight Airfoil Configurations at +2 Degrees Angle of Attack	52
26	The Effect of C_{μ} on l/d for Eight Airfoil Configurations at +4 Degrees Angle of Attack	53
27	The Effect of C_{μ} on l/d for Eight Airfoil Configurations at +6 Degrees Angle of Attack	54

List of Tables

<u>Table</u>		<u>Page</u>
I	Airfoil Configurations	30

List of Symbols

α_g	Geometric angle of attack, degrees
c	Model chord length, feet
C_{p_l}	Pressure coefficient on the lower surface of the airfoil
C_{p_u}	Pressure coefficient on the upper surface of the airfoil
C_{d_o}	Section profile drag coefficient
C_{d_t}	Section total drag coefficient, $C_{d_o} + C_\mu$
C_l	Section lift coefficient, $C_n \cos \alpha_g$
C_n	Section normal force coefficient, $N/q_o c$
C_μ	Momentum coefficient, $\dot{m} V_j / q_o c$
l/d	Section lift-to-total drag ratio
\dot{m}	Mass flow rate of blowing air per unit span, lbm/sec/ft
N	Normal force per unit span, lb _f
q	Local dynamic pressure, psfg
q_o	Free stream dynamic pressure, psfg
Re	Reynolds number, based on chord, $\frac{\rho V C}{\mu}$
V_j	Velocity at the slot, ft/sec
V_o	Free stream velocity, ft/sec

Abstract

Wind tunnel tests were conducted to determine the effects of trailing edge modifications on the lift-to-drag ratio of a circulation controlled airfoil. The model was a 20 percent thick, five percent cambered, elliptical airfoil. The airfoil was modified in aft contour, blowing slot position, and blowing angle. A 1.5 inch splitter plate was mounted at the 99 percent chord for all tests. The tests were run at a Reynolds Number, based on model chord, of 7.41×10^5 , while the angle of attack and blowing rate were varied during each test sequence.

It was found that the modifications caused increases in the section lift coefficient and decreases in the section total drag coefficients as compared to the original airfoil. Due to these results, the lift-to-drag ratio for airfoils using modifications were higher than the original airfoil. A comparison of the results for these modified airfoils revealed that there were no drastic differences due to the modifications. This indicated that the changes made provided for little variation in results, and that such changes needed to be of greater magnitude.

A WIND TUNNEL STUDY OF THE EFFECTS OF
TRAILING EDGE MODIFICATIONS ON THE
LIFT-DRAG RATIO OF A CIRCULATION
CONTROLLED AIRFOIL

I. Introduction

In recent years, there has been renewed interest in the area of low-speed, high-lift flight. This has been derived through the need for short take-off and landing aircraft. This concept has many applications. They range from the missions of reconnaissance aircraft to those of low-speed, high-lift transports.

One method for obtaining high lift at low speeds is through circulation control. Circulation control on an airfoil is a process of delaying flow separation through the use of a jet of air. A blowing slot placed near the trailing edge of the airfoil acts to re-energize the boundary layer and move the front and rear stagnation points to the lower surface of the airfoil. This movement of the stagnation points results in an increase in the section lift coefficient, C_l , and a decrease in the section profile drag coefficient, C_{d_0} .

Previous Studies

Through the use of an uncambered elliptical airfoil, Kind (Ref 3) obtained section lift coefficients of 3.2. Following this, the studies

of Williams (Ref 7), Walters (Ref 6), and Englar (Ref 2) produced even higher lift coefficients.

Stevenson (Ref 5), in following a recommendation by Kind, investigated the feasibility of using a splitter plate to obtain greater lift to drag ratios (l/d) through a reduction in mixing losses.

Stevenson used a 20 percent thick, five percent cambered airfoil in his study. From his study, Stevenson obtained a maximum l/d of 56 with a splitter plate of 1.5 inch chord.

Rhynard (Ref 4) continued the work of Stevenson by investigating the optimum splitter plate position and angle for maximum l/d . Rhynard obtained a maximum l/d with the splitter plate at the 99 percent chord position and at a 45 degree angle. He also found that a splitter plate in the 95.3 percent chord position yielded a maximum l/d when set at a 60 degree angle.

Present Study

The objective of this study was to investigate the effect of trailing edge modifications on the airfoil tested by Stevenson and Rhynard. Through changes in the trailing edge contour, and blowing slot position and angle, the effects of such variables could be observed and trends determined for future research. It is important to see such results in order to produce an optimal airfoil for low-speed, high-lift flight.

Scope

The study consisted of several segments. The first segment was the determination of which airfoil modifications should be observed and the submission of plans for such modifications. Consideration was given to those variables which, through past studies, had shown to be influential in the performance of an airfoil. Therefore, modifications in the aft contour, blowing slot position, and blowing slot angle were made.

The second segment of the study was to test the model and its modifications in the Air Force Institute of Technology's Five Foot Wind Tunnel. The tests were run at a Reynolds number of 7.41×10^5 and at a range of momentum coefficients from 0.0 to 0.045. The tests were conducted with a 1.5 inch splitter plate and through a range of geometric angles of attack from -6 to +6 degrees. The splitter plate was located at the 99 percent chord position at a 45 degree angle.

The final segment of the study was a flow visualization study through the use of tufts. The tuft studies were made at a momentum coefficient of 0.03 for the various angles of attack.

II. Description of Apparatus

Wind Tunnel

The wind tunnel tests were conducted in the Air Force Institute of Technology's Five Foot Wind Tunnel. It is an open return, closed test section wind tunnel with a maximum speed of 250 miles per hour empty. A two-dimensional test section was simulated by the installation of two wooden side boards resulting in a 60 inch by 30 inch tunnel cross section. Two-dimensional flow characteristics were enhanced by the attachment of circular, beveled endplates to each end of the airfoil. The secondary air source was obtained from a separate compressed air supply.

Airfoil

The experimental airfoil, shown in Fig. 1, was a 20 percent thick, five percent cambered, elliptical airfoil, symmetrical about the front and rear. The model, designed for use with interchangeable trailing edges, had a span of 2.17 ft and a chord of 1.67 ft. There were 48 static pressure taps distributed along the upper and lower surfaces of the airfoil.

The secondary air was brought into the airfoil through a copper pipe which directed the air to a fiberglass plenum chamber. The chamber was of diverging-converging cross section, and extended along the entire span of the airfoil. The 0.02 inch blowing slot

represented the minimum area to which the chamber converged. The slot provided blowing air to the upper rear surface of the airfoil. Additional information concerning the airfoil design can be found in Stevenson's report (Ref 5:11).

Airfoil Modifications

Previous studies had shown that the trailing edge contour, the location of the blowing slot, and the angle at which the air entered the flow were important variables when dealing with high lift devices. It was feasible to modify the original airfoil in all three of these areas. The modifications yielded eight different configurations which were combinations of original and new design features.

The blowing slot location of the original airfoil was the 96 percent chord position. Adequate results were previously obtained at this location, however, it was desired to investigate the effect of a movement of the slot. Consequently, the slot location was moved to the 97 percent chord position on four of the eight configurations. The choice in moving the slot rearward was arbitrary, but did provide an opportunity to investigate the effect of the adverse pressure gradient should it exist in that area.

The airfoil used by Rhynard was designed with a blowing angle of approximately 5 deg. from the horizontal. Through the use of a step between the upper and lower slot edges, see Fig. 2, an angle of approximately -33 deg. was obtained. This allowed the air to

enter more tangential to the surface than in the original case. This angle was used on four configurations.

Previous studies had shown that the shape of the trailing edge greatly affected lift and drag values for circulation controlled airfoils (Ref 2). In order to investigate this, four of the configurations employed a rounded trailing edge ($r = 0.95$ inches) as opposed to the original elliptical design. The 0.95 inch radius was chosen so as not to change the overall chord length of the model.

For comparison purposes, one configuration was designed with all of the original features, and one configuration included all of the new features. The remaining six configurations were combinations and can be found in Table I.

Each of the configurations was grooved for use with a splitter plate as described by Rhynard. Additionally, the same 1.5 inch splitter plate was used for all tests (Ref 4:5). The splitter plate was located at the 99 percent chord position at a 45 degree angle. In the remaining discussion, this position will be referred to as the B position and the configurations will be referred to by the numbers one through eight as they appear in Table I.

Pitot Tube Apparatus

The pitot tube apparatus was used to measure the spanwise pressure distribution along the blowing slot in order to determine flow uniformity. The apparatus was the same as described by

Rhynard (Ref 4:6) with the exception of the tube used. The tangential angle of four of the configurations required that the two inch tube be bent so as to point directly into the slot at each spanwise point. The diameter of the tube was 0.02 inches. The other four configurations employed a straight tube in recording the spanwise pressure readings.

Flowmeter

A 0.5 inch throat diameter venturi tube was used to obtain the mass flowrate of the secondary air. A pressure reading was taken from a flange tap at the throat and a tap upstream of the throat. The temperature was measured with a copper-constantan thermocouple which was located upstream from the venturi throat.

Oil Filter

Rhynard's study indicated that the oil and water contained in the secondary air was a heavy influence on his results. Because of this, a filtering system, as shown in Fig. 4, was used to eliminate the oil and water. The filter was located upstream of the venturi and consisted of a diverging cone, a cylindrical settling chamber, and a converging cone. The initial cone diverged at a half angle of seven degrees in order to slow the flow without causing separation. The flow was slowed, allowing the oil and water to settle in the chamber before the air passed through a filter which was placed between the settling chamber and the converging cone.

Wake Survey Rake

A total head wake survey rake was used to measure the momentum deficit of the airfoil wake. The rake consisted of two static pressure tubes and 96 total head tubes. The tubes were spaced 0.25 inches apart and were 0.0625 inches in diameter. The rake was located 1.85 chord lengths behind the airfoil. The complete rake assembly spanned the entire test section from top to bottom with the rake itself adjusted as close to the tunnel floor as possible.

Manometers

The wake survey rake was connected to a 100 tube, red oil manometer bank of which 98 tubes were utilized. In order to obtain more accurate readings, the manometer bank was inclined 30 degrees from the vertical. Fifty tubes of a vertical alcohol manometer bank were utilized to measure the static pressures along the surface of the airfoil, and the free stream and test section dynamic pressures. The total pressure in the plenum chamber was measured on three tubes of a six tube, 50 inch mercury manometer board. Finally, two 60 inch mercury manometers were used to measure the pressures across the venturi tube.

III. Experimental Procedures

Following installation of the equipment, the airfoil was calibrated for angle of attack. After the calibration, the secondary air system and oil filter were checked for leaks. Finally, the equipment used for measurements was checked for proper operation. The testing began with the attachment of an endpiece to the airfoil. The splitter plate was then assembled onto the airfoil. As the tunnel was brought to speed, 74 feet per second, a predetermined venturi pressure was set. Due to a time lag between the tunnel and the manometers, it was necessary to allow sufficient time for the manometers to adjust to tunnel conditions. After this, the geometric angle of attack was varied from -6 degrees to +6 degrees. The sequence commenced at 0 degrees and proceeded in order to -6 degrees to +6 degrees at two degree intervals. A final reading was taken at 0 degrees in order to check repeatability of data.

At each of the angles of attack, the manometer banks were photographed and the plenum chamber total pressure and venturi pressures recorded. Once the angle of attack sequence was completed, the blowing rate via the venturi pressures was changed and the angle of attack sequence was repeated. Once the procedure was completed for four blowing rates, the configuration was changed by attaching a new endpiece. This entire procedure was repeated until all eight configurations had been tested. Finally, re-tests were made

to check for accuracy and spanwise pressure distributions were made for each configuration. The filters in the secondary air system were changed after every four runs. In addition, a limited tuft study was performed on each configuration to check for separation and two-dimensionality of flow.

IV. Data Reduction

Section Lift Coefficient

The section lift coefficient, C_l , was calculated according to the following equation:

$$C_l = C_n \cos \alpha_g \quad (1)$$

In the above equation, C_n is the section normal force coefficient and α_g is the geometric angle of attack (Ref 4:9). C_n was found by numerical integration of the pressure coefficients around the airfoil. The Hewlett-Packard 9100A Calculator and 9107A Digitizer employed the trapezoidal rule in performing the integration. The integration was performed according to the equation

$$C_n = \int_0^1 (C_{p_l} - C_{p_u}) d \left(\frac{x}{c} \right) \quad (2)$$

where C_{p_l} and C_{p_u} are the pressure coefficients on the lower and upper surfaces respectively, and $\left(\frac{x}{c} \right)$ is the chordwise distance along the airfoil (Ref 4:9).

Momentum Coefficient

The amount of blowing applied to a circulation controlled airfoil is represented by the momentum coefficient, C_μ . The momentum coefficient was calculated by the following equation:

$$C_{\mu} = \frac{\dot{m} V_j}{q_o c} \quad (3)$$

In this equation, \dot{m} is the mass flowrate of blowing air per unit span, V_j is the velocity of the air at the blowing slot, q_o is the free stream dynamic pressure, and c is the airfoil chord length (Ref 4:9).

Section Total Drag Coefficient

The section profile drag coefficient, C_{d_o} , was calculated from the equation

$$C_{d_o} = \frac{2}{c} \int_0^h \left(\sqrt{\frac{q}{q_o}} - \frac{q}{q_o} \right) dy + \frac{\dot{m} V_o}{q_o c} \quad (4)$$

where q and q_o are the dynamic pressures in the wake and free stream respectively, and dy is the incremental distance between tubes on the wake survey rake. In the second term, \dot{m} is the mass flowrate, V_o is the free stream velocity, and c is the airfoil chord length (Ref 4:10). The integral term of Eq (4) was found by integration on the Hewlett-Packard calculator and digitizer.

The section total drag coefficient was calculated by the equation

$$C_{d_t} = C_{d_o} + C_{\mu} \quad (5)$$

where C_{d_o} is the section profile coefficient and C_{μ} is the momentum coefficient (Ref 4:10). The second terms of Eqs (4) and (5) are included for the purpose of comparing a circulation controlled airfoil

with an unblown airfoil. When blowing is applied, the momentum theory requires that these terms be added to the section profile drag because they decrease the momentum deficit measured by the wake survey rake. The second term of Eq (4) represents the intake penalty coefficient which would be necessary to obtain air for blowing. The actual drag of the airfoil used in this study would not include this term, however, it is necessary to include it in order to compare this airfoil with unblown airfoils. The second term of Eq (5) is the momentum coefficient and must be added because the blowing results in a decrease in the momentum deficit and, consequently, the drag measured is not the actual drag of the airfoil. This term is also necessary in that it represents momentum which originates inside the model or outside the system as is the case with a secondary air source of the sort used in this study.

A quick summary shows that the second terms of Eqs (4) and (5) are necessary to obtain a true measure of the momentum deficit, and to compare drag results with unblown airfoils.

Lift-to-Drag Ratio

The lift-to-drag ratio, l/d , is the ratio of the section lift coefficient to the section total drag coefficient. It was calculated according to the following equation:

$$l/d = C_l / C_{d_t} \quad (6)$$

Wind Tunnel Corrections

Standard two-dimensional solid and wake blocking corrections were applied to C_l , C_{dt} , q_o and R_e . Additionally, a streamline curvature correction was applied to C_l .

V. Results and Discussion

General Observations

Through the use of the oil filtering system, the adverse effect of the buildup of oil and water was eliminated. Without the effect of oil, it was possible to observe the separation tendencies of the various configurations. Rhynard's study indicated that separation often occurred at +4 to +6 degrees angle of attack for blowing rates less than 0.05 (Ref 4:13). The blowing rates for the present study were all less than 0.05 and allowed an investigation of this occurrence. This study indicated that separation occurred from +1 to +5 degrees angle of attack. The effect of angle of attack on C_l , C_d , and l/d can be seen in detail in deJonckheere's report (Ref 1).

Due to problems in design, the 1-B configuration's slot width varied as blowing was applied. With an increase in C_μ , the slot width increased and consequently, the results for 1-B do not follow the trends set by the other configurations. The effect of this slot width variation can be seen in Figs. 5 through 27.

The spanwise pressure surveys indicated that the flow from the slot was essentially uniform on the various endpieces. However, the flow for configuration 2-B was not uniform. The data for this configuration is presented in order to show the effect of the non-uniform flow on the lift-to-drag ratio. The pressure surveys of the other endpieces indicated that the flow was uniform from endplate to

endplate. At the higher blowing rates, some flow variation was noted near the endplate.

The tuft study revealed that some vorticity was present near the endplates. This showed that complete two-dimensional flow was not achieved. This study also indicated that the flow was essentially two-dimensional across the mid-span or the region in which measurements were made. The study also showed that flow attachment increased with blowing, and that separation occurred at the higher angles of attack.

Lift Results

The lift results are presented in Figs. 5 through 11. All eight configurations are shown in each figure in order to obtain trends for the various configurations. The section lift coefficient increased as the momentum coefficient increased. The maximum values for C_l increased as the angle of attack increased toward separation. Comparison of the figures revealed that the maximum lift coefficients were less than 2.0 at -6 degrees angle of attack, that they had risen to about 2.5 at 0 degrees angle of attack, and reached their peak at +2 to +4 degrees angle of attack. In conjunction with this, Figs. 9 through 11 show the effect of separation on the section lift coefficient. The values at $C_\mu = 0.0$ were close, but when blowing was applied, several differences were noted. As shown in Figs. 5 through 9, all endpieces with new design features yielded higher section lift coefficient than the original design. However, some values for the 1-B

configuration were higher for C_{μ} 's near 0.04 and for +6 degrees angle of attack. These exceptions were attributed to separation and to 1-B's variation in slot width as blowing was applied.

Direct comparisons of the effects of modifications were not possible due to the closeness of the results. In many cases, the difference in results for various configurations was within experimental error and thereby prevented an accurate evaluation of the configurations. Therefore, the modifications had to be reviewed in terms of trends. One definite trend which developed was that configuration 4-B yielded the highest section lift coefficients for this study. This configuration employed the tangential blowing angle, and the circular contour with the slot located at the 96 percent chord.

Fig. 10 shows that 4-b achieved a maximum lift coefficient of 2.68 at a momentum coefficient of 0.043 and +4 degrees angle of attack. The 3-B and 5-B configurations achieved relatively high section lift coefficients at the lower blowing rates but tended to reach their peak at $C_{\mu} = 0.04$. This was attributed to the combination of the slot position and aft contour on each of these configurations.

Figure 6 shows that the 6-B, 7-B, and 8-B configurations obtained lift coefficients that were lower than the 4-B configuration. Since these configurations were combinations of at least two modifications, it had been anticipated that they would yield section lift coefficients comparable to 4-B. These configurations employed a 97

percent chord slot position, and their inability to achieve higher lift coefficients was attributed to the slot being in the adverse pressure gradient and unable to provide the boundary layer control necessary for high section lift coefficients. It also indicated that the modifications might not have been mutually benefitting when in combination.

The 2-B endpiece is not discussed due to non-uniformity of flow. The results are presented in the figures for observation.

The effectiveness of the contour change and angle change have not been discussed due to relatively small differences in the results for configurations employing these modifications. However, 4-B employed both of these modifications and indicated that the contour and angle change were effective when in combination.

In summarizing the lift results, it is important to note that the results for all the configurations were close and made it necessary to look at the effects of the modifications in terms of trends. Figs. 5 through 9 reveal that the curves are close and that a quantitative and qualitative comparison between endpieces was impractical. However, 4-B was generally superior and yielded the highest lift coefficients. The other configurations which figured to yield high lift coefficients were affected by the slot position and adverse pressure gradient. The modifications did, however, increase the lift coefficients over the original design.

Drag Results

The graphs of drag coefficient versus momentum coefficient, shown in Figs. 12 through 20, represent the drag results. The data reduction methods used to determine drag were very sensitive and provided considerably more experimental error than is normal. This affected the ability to accurately evaluate the effects of the modifications and forced an evaluation of trends rather than specifics. The figures show that, in most cases, the configurations with modifications were effective in reducing the drag as compared to the original airfoil. The figures also show that the total drag increased as the momentum coefficient increased. This was caused by the increase in C_{μ} . The profile drag coefficient, C_{d_0} , actually decreased with blowing as shown in Figs. 19 and 20. Figs. 16 through 18 show the effects of separation on drag, and that different configurations separated at different angles of attack.

Figs. 13 through 15 reveal that the 4-B configuration yielded the lowest drag at zero blowing and for the very low blowing rates. At moderate to high rates of blowing, the 3-B configuration maintained lower drag levels while 4-B increased to higher values. The only difference between 3-B and 4-B was that 4-B employed the tangential angle while 3-B employed the original angle. This indicated that the tangential angle was of little benefit in this case. An inspection of the drag values for 6-B showed that the new angle, in combination with the elliptical contour, was effective in reducing drag as

compared to other configurations employing the 97 percent chord slot position. Some of this reduction in drag is attributed to the elliptical contour which, through previous studies, yielded lower drag values than a circular contour. This result, coupled with the observations made on 3-B and 4-B, indicated that the new angle might have had some effect in drag reduction, but the results did not provide ample evidence to accurately determine the effect of the angle.

The elliptical contour yielded its best results when used in combination with the 97 percent chord slot position as evidenced by a comparison of 5-B and 6-B. The latter had, in general, lower drag values than did 5-B. Additionally, the best results obtained with a 96 percent chord slot location were with 3-B and 4-B which employed the circular contour.

Lift-to-Drag Results

The lift-to-drag results are presented in Figs. 21 through 27. Based on its ability to maintain low values for drag and fairly high values for lift, 3-B consistently yielded the best l/d results, as shown in Figs. 22 through 24. This configuration obtained an l/d of 46.41 which was the maximum for this study. 7-B and 6-B yielded the second and third highest values for l/d respectively. Of all eight configurations, the 3-B, 4-B, and 6-B configurations were the most consistent in obtaining high l/d values. This was true for zero degrees and negative angles of attack. Due to separation effects,

7-B and 8-B obtained the highest l/d values at +2 degrees angle of attack while the results at +4 and +6 degrees angle of attack are inconclusive.

The effect of blowing was seen in the results for 4-B and 6-B. The figures show that 4-B yielded the highest l/d values at $C_\mu = 0.0$, but did not increase as rapidly as 3-B when blowing was applied. In addition, 6-B consistently obtained high values for l/d at moderate blowing rates, but rapidly decreased as blowing continued to increase. In conjunction with this, it was found that seven configurations obtained their maximum l/d values at 0 to +2 degrees angle of attack and at blowing rates of 0.018 to 0.03. Higher blower rates resulted in a decrease in l/d .

Trends which evolved from these observations showed that the circular contour was effective in increasing l/d when used with the 96 percent chord slot position. This is seen in the performance of configurations 3-B and 4-B. This also indicated that the new slot angle had little effect on the l/d values. In the case of configuration 6-B, the new slot angle seemed effective in producing high l/d values. This is attributed to the ability of the new angle to help overcome the effects of the adverse pressure gradient. By comparison with 8-B, it was found that this angle was most beneficial when used with the elliptical contour. This seemed to be the only case where the 97 percent chord slot position was beneficial.

VI. Conclusions

A two-dimensional wind tunnel study to determine the effects of trailing edge modifications on the lift-to-drag ratio of a circulation controlled airfoil resulted in the following conclusions.

1. The section lift coefficient is a maximum when in use with a 96 percent chord slot position and a circular aft contour.
2. The section total drag coefficient is a minimum when the circular contour is combined with the 96 percent chord slot position and when the elliptical contour is combined with the 97 percent chord position.
3. The section lift-to-drag ratio was a maximum for angles of attack near zero degrees.
4. The section lift-to-drag ratio is a maximum for all configurations when the momentum coefficient is between 0.018 and 0.03.
5. Airfoils employing the 96 percent chord slot position, yielded a maximum section lift-to-drag ratio when in combination with the circular contour.
6. Airfoils employing the 97 percent chord slot position, yielded a maximum section lift-to-drag ratio when in combination with the elliptical contour and the tangential angle.

VII. Recommendations

It is recommended that further wind tunnel tests of circulation controlled airfoils include:

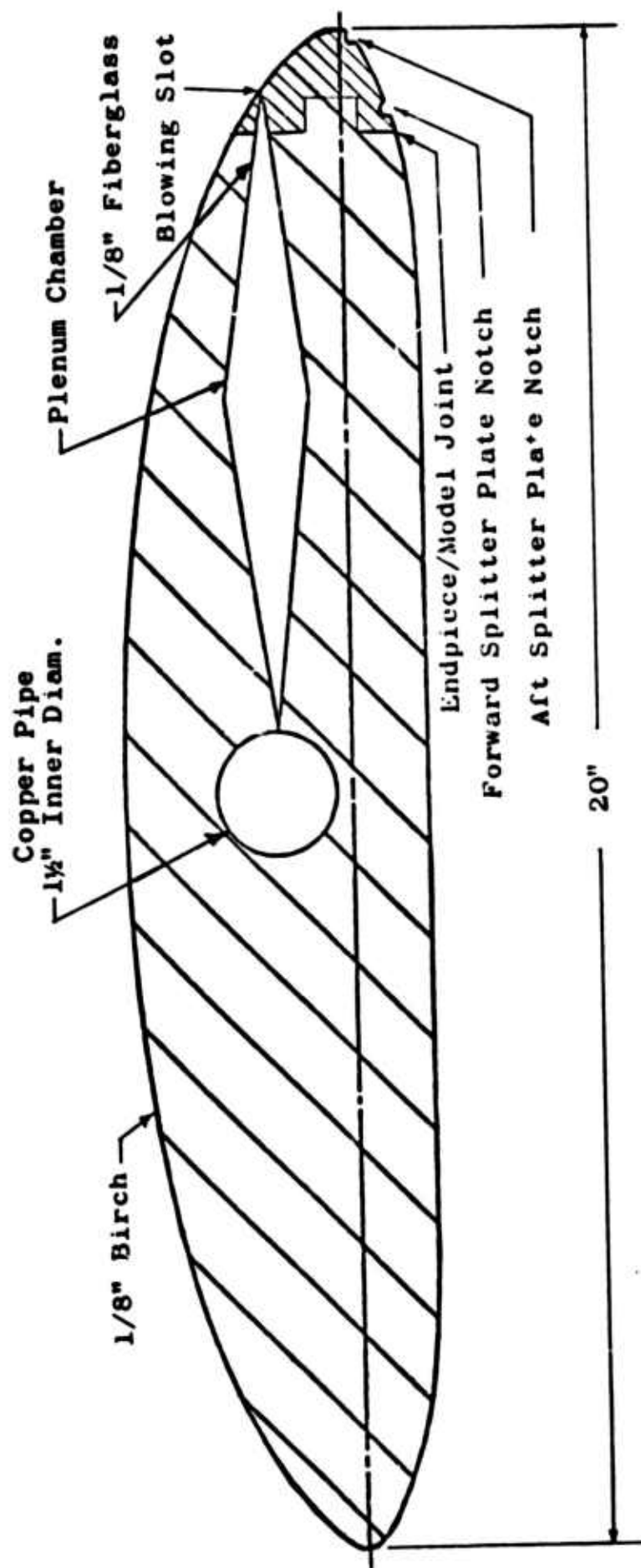
1. A lengthening of the wake survey rake so as to cover a greater section of the tunnel and result in more accurate drag measurements.
2. A determination of a less sensitive method for reducing drag pressure data.
3. A detailed investigation of changes in slot position by means of forward and aft changes from the 96 percent chord position.
4. A determination of the effect of slot width on the lift-to-drag ratio.

Bibliography

1. deJonckheere, R. K. An Analytic and Experimental Study of the Effects of Splitter Plate Position on the Trailing Edge Modifications of a Cambered Circulation Controlled Elliptical Airfoil. Unpublished Thesis. Wright-Patterson Air Force Base, Ohio: Air Force Institute of Technology, 1975.
2. Englar, R. J. Two-Dimensional Subsonic Wind Tunnel Tests of Two 15-Percent Thick Circulation Control Airfoils. NSRDC Technical Note AL-211. Bethesda, Maryland: Naval Ship Research and Development Center, 1971. AD 900210.
3. Kind, R. J. A Proposed Method of Circulation Control. Unpublished Ph. D. Dissertation. University of Cambridge, England: Aeronautical Engineering Department, 1967.
4. Rhynard, W. E. A Wind Tunnel Study of the Effects of Splitter Plate Position and Angle on the Lift-Drag Ratio of a Circulation Controlled Elliptical Airfoil. Unpublished Thesis. Wright-Patterson Air Force Base, Ohio: Air Force Institute of Technology, 1974.
5. Stevenson, T. A. A Wind Tunnel Study of the Lift-Drag Ratio on a Cambered Circulation Controlled Elliptical Airfoil. Unpublished Thesis. Wright-Patterson Air Force Base, Ohio: Air Force Institute of Technology, 1974.
6. Walters, R. E., et al. Circulation Control by Steady and Pulsed Blowing for a Cambered Elliptical Airfoil. NR 215-163. Morgantown, West Virginia: West Virginia University, 1972. AD 751045.
7. Williams, R. M., and H. J. Harvey. Two Dimensional Subsonic Wind Tunnel Tests on a 20 Percent Thick, 5 Percent Cambered Circulation Control Airfoil. NSRDC Technical Note AL-176. Washington, D. C.: Naval Ship Research and Development Center, 1970. AD 877764.

Appendix A

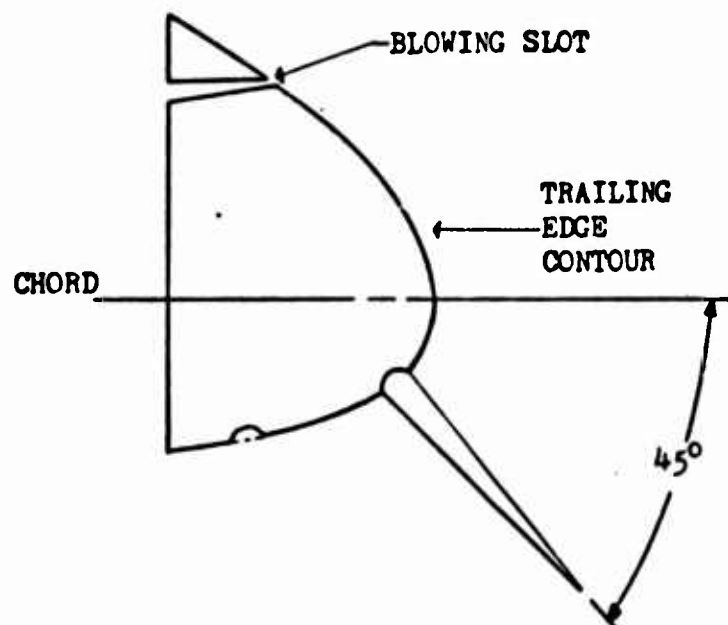
Apparatus



Scale 1"=2 1/4"

Fig. 1 Cross Section of the Airfoil With Endpiece Attached

CONFIGURATION 1-B
SLOT POSITION = $96\% \bar{c}$
SLOT ANGLE = 5 Deg.
ELLIPTICAL CONTOUR



CONFIGURATION 2-B
SLOT POSITION = $96\% \bar{c}$
SLOT ANGLE = -33 Deg.
ELLIPTICAL CONTOUR

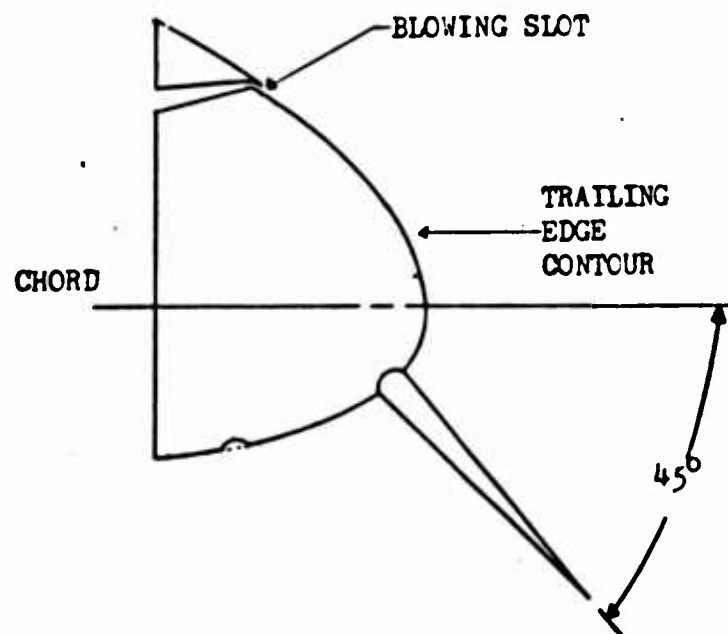
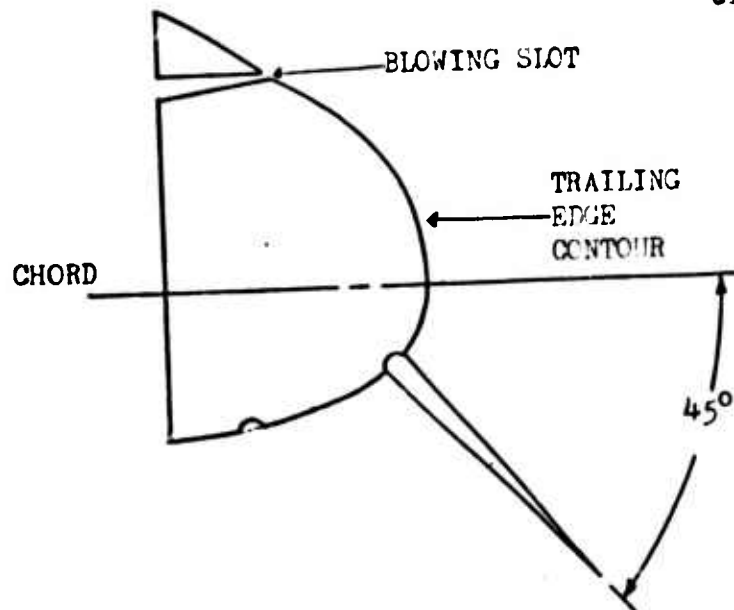


Fig. 2. Trailing Edge Configurations 1-B and 2-B

CONFIGURATION 3-B
SLOT POSITION = $96\% \bar{c}$
SLOT ANGLE = 5 Deg.
CIRCULAR CONTOUR



CONFIGURATION 5-B
SLOT POSITION = $97\% \bar{c}$
SLOT ANGLE = 5 Deg.
ELLIPTICAL CONTOUR

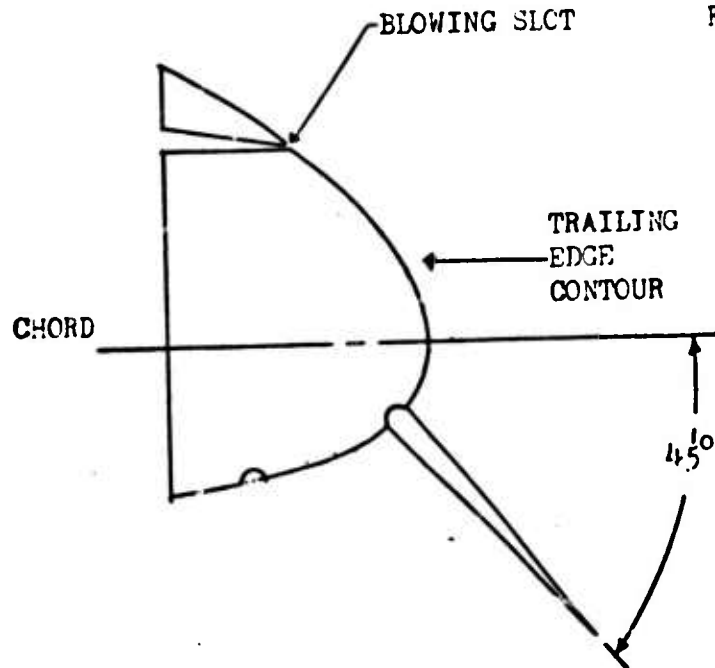


Fig. 3. Trailing Edge Configurations 3-B and 5-B

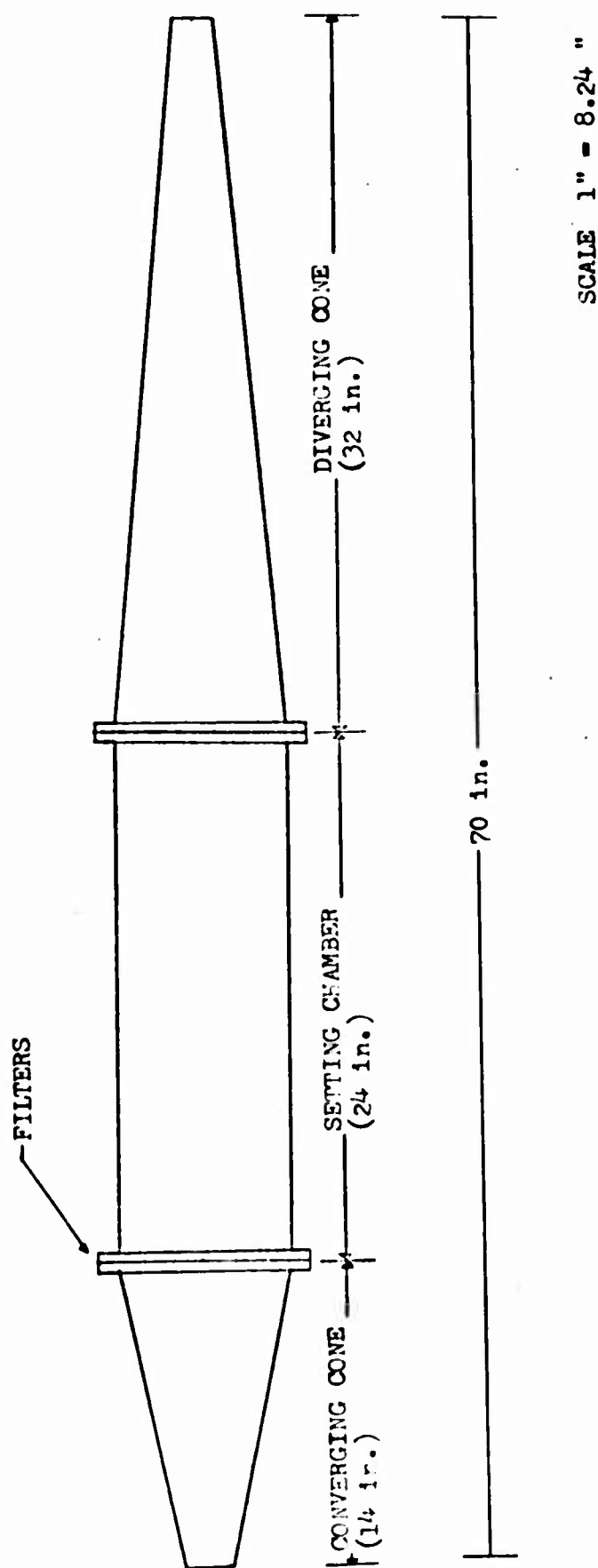


Fig. 4. OIL FILTERING SYSTEM

Table I
Airfoil Configurations

Configuration	Contour	Slot Position	Slot Angle
1-B*	Elliptical	96% c	5 deg
2-B**	Elliptical	96% c	-33 deg
3-B	Circular	96% c	5 deg
4-B	Circular	96% c	-33 deg
5-B	Elliptical	97% c	5 deg
6-B	Elliptical	97% c	-33 deg
7-B	Circular	97% c	5 deg
8-B	Circular	97% c	-33 deg

Splitter Plate:

Length - 1.5 in.
Deflection Angle - 45°
Location - 99% chord

*Defective due to slot width variation

**Defective due to non-uniformity of flow at the slot.

Appendix B

Data

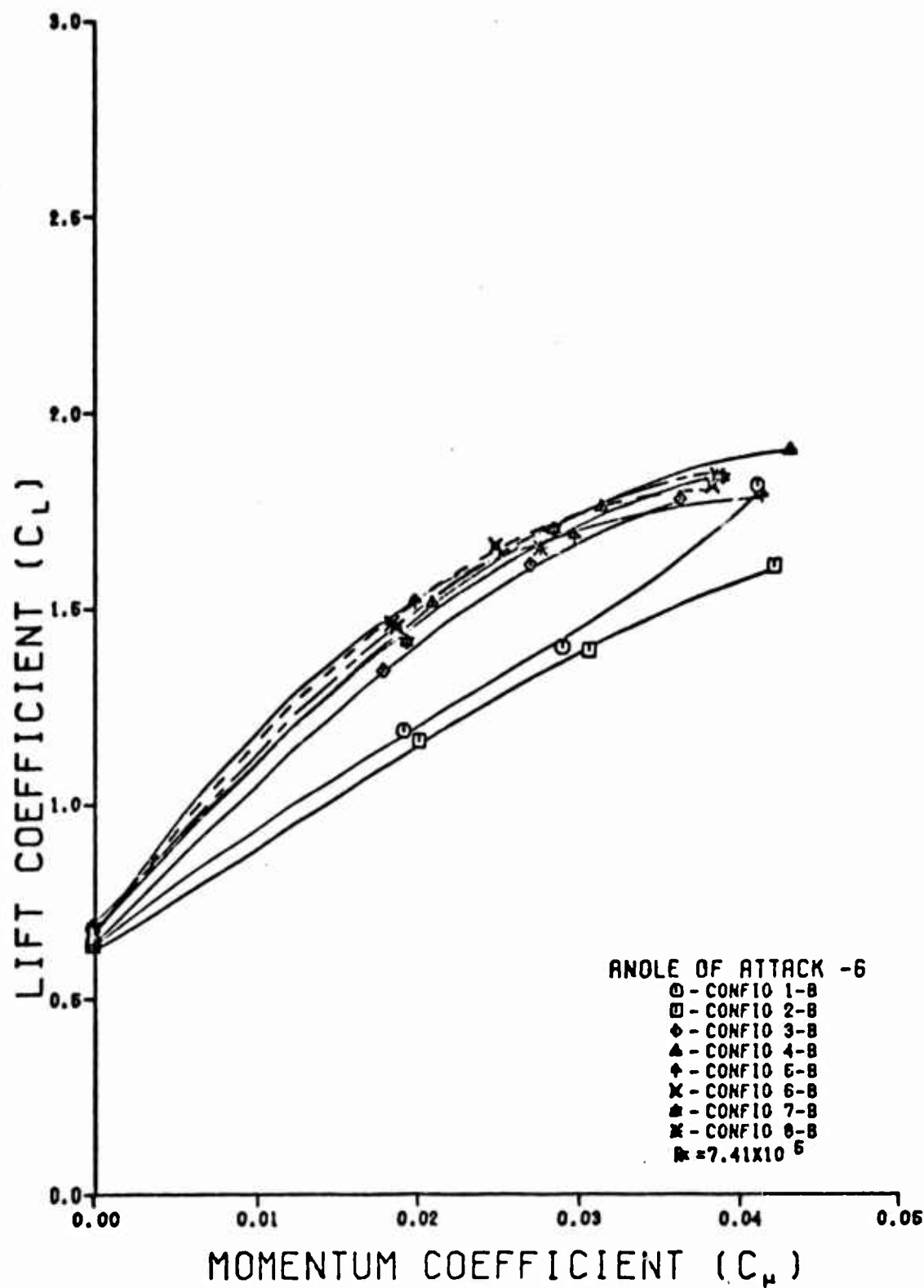


Fig. 5. The Effect of C_{μ} on C_l for Eight Airfoil Configurations at -6 Degrees Angle of Attack

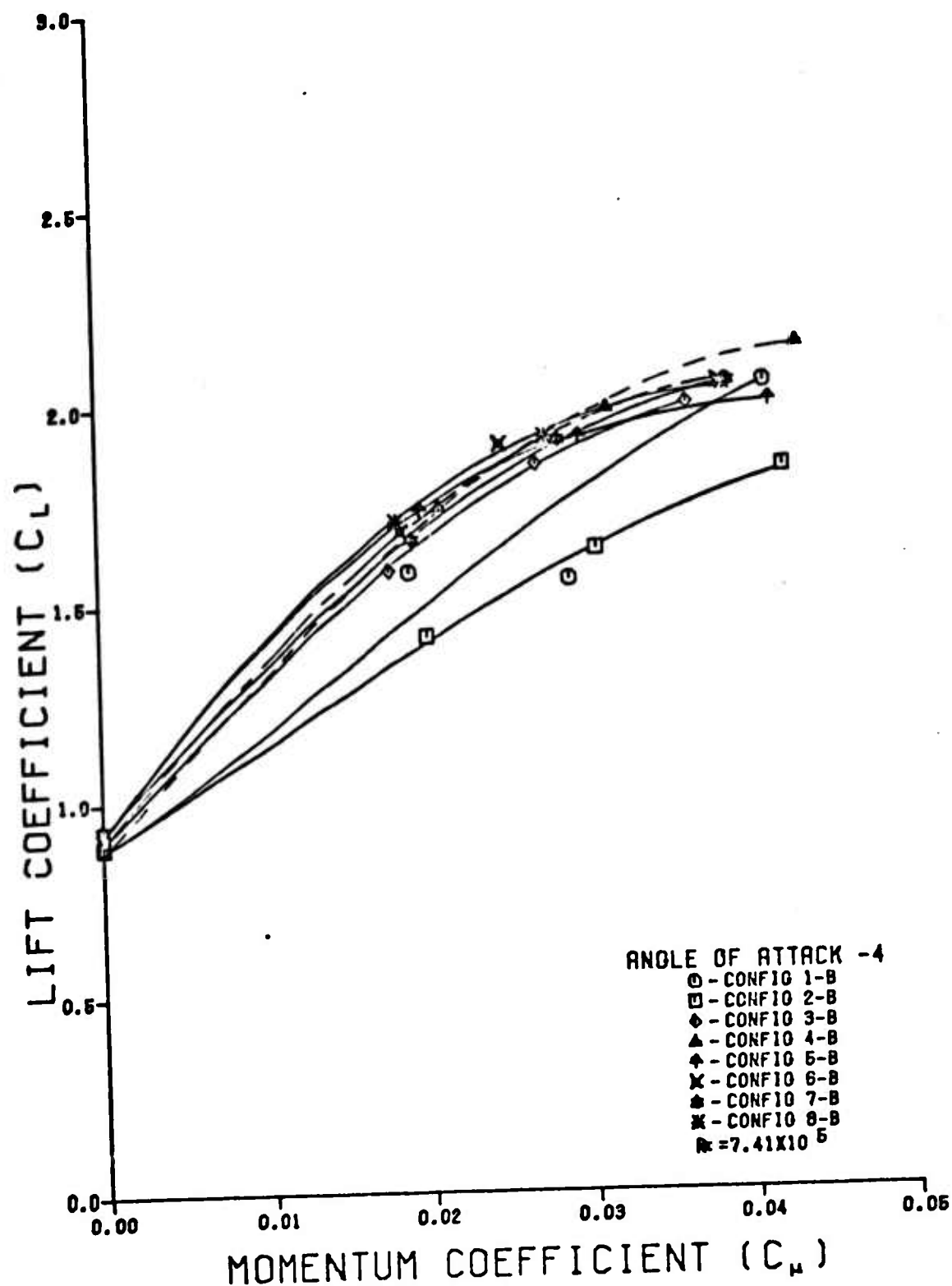


Fig. 6. The Effect of C_{μ} on C_l for Eight Airfoil Configurations at -4 Degrees Angle of Attack

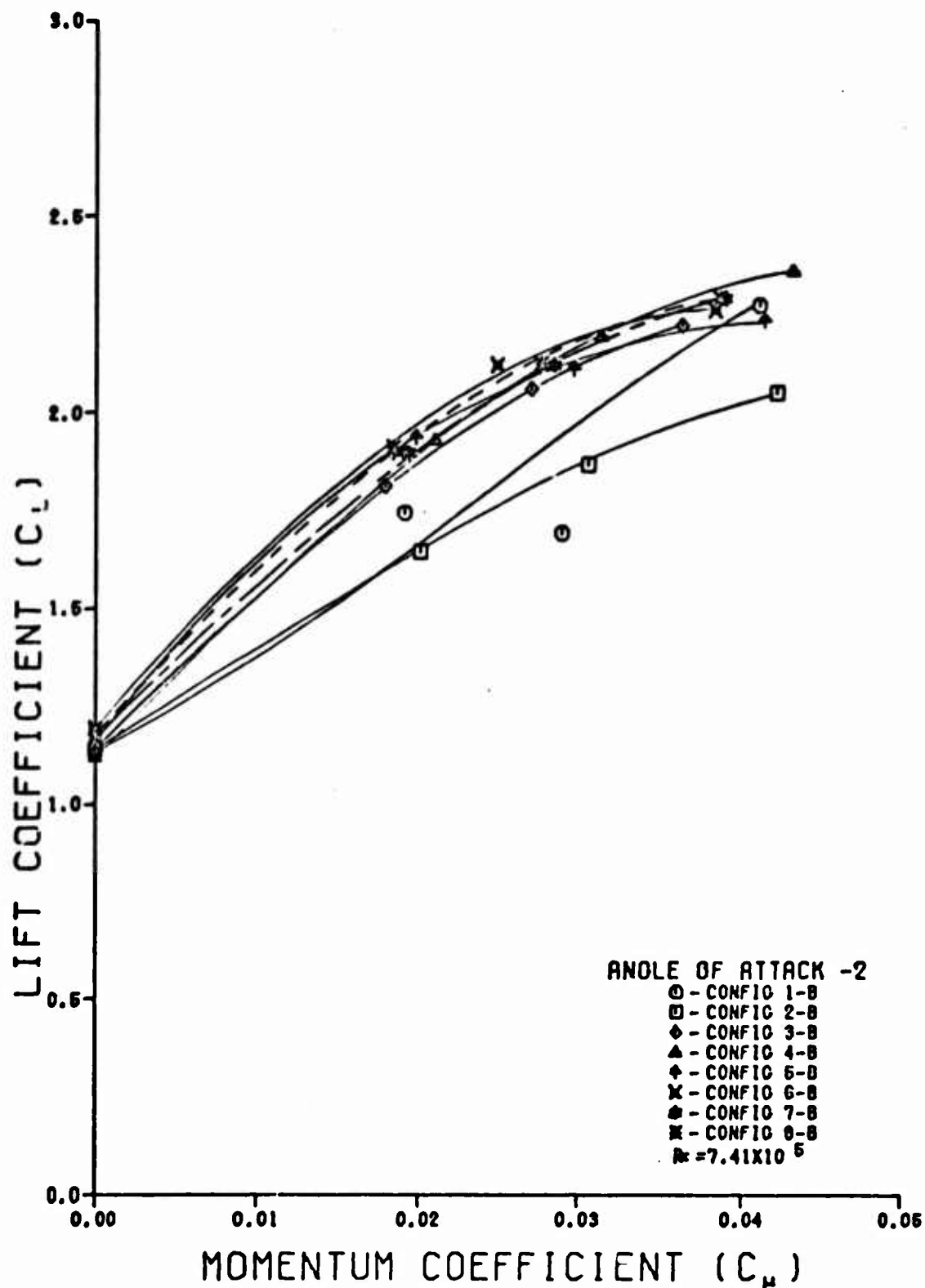


Fig. 7. The Effect of C_{μ} on C_L for Eight Airfoil Configurations at -2 Degrees Angle of Attack

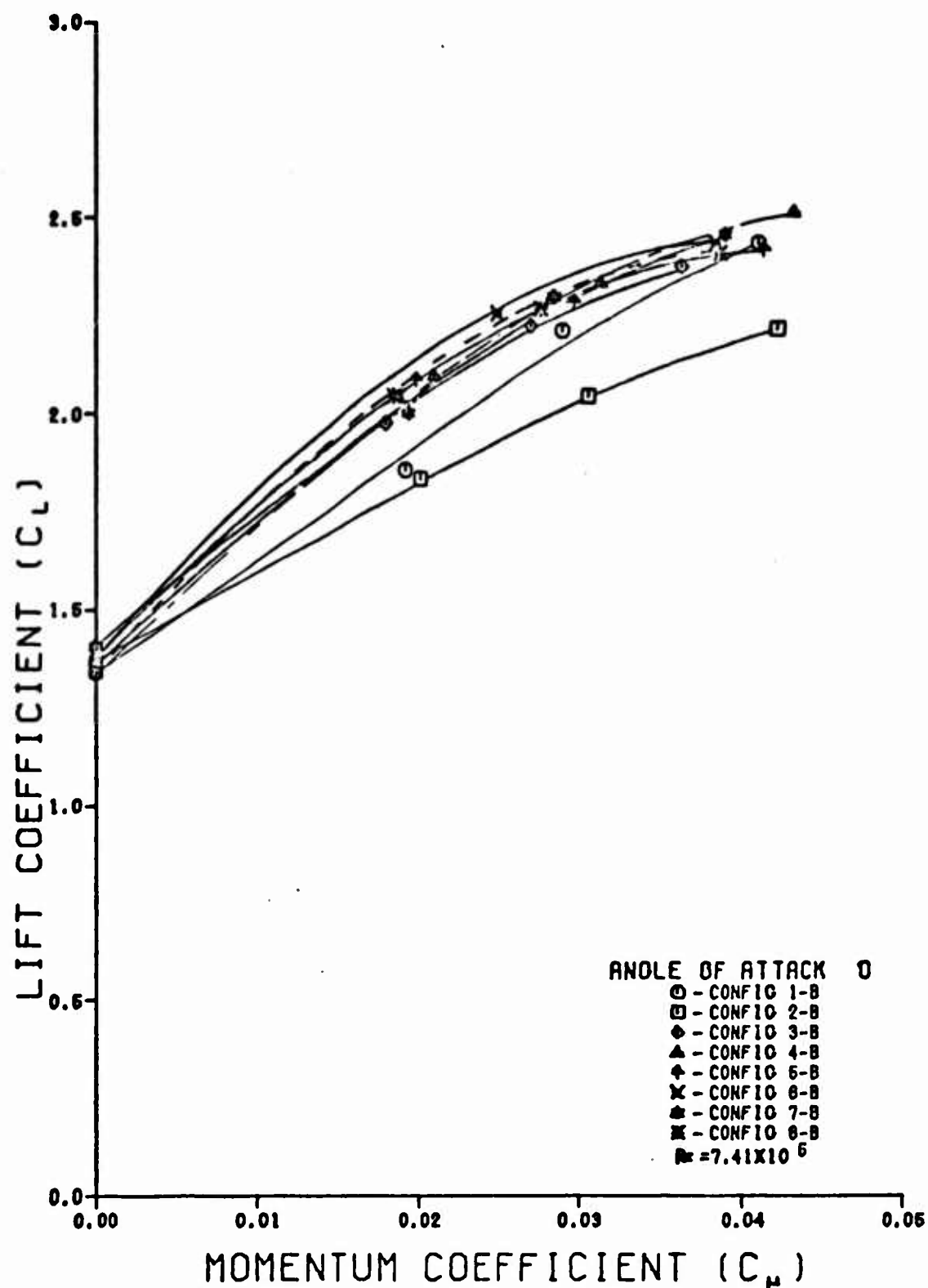


Fig. 8. The Effect of C_{μ} on C_L for Eight Airfoil Configurations at 0 Degrees Angle of Attack

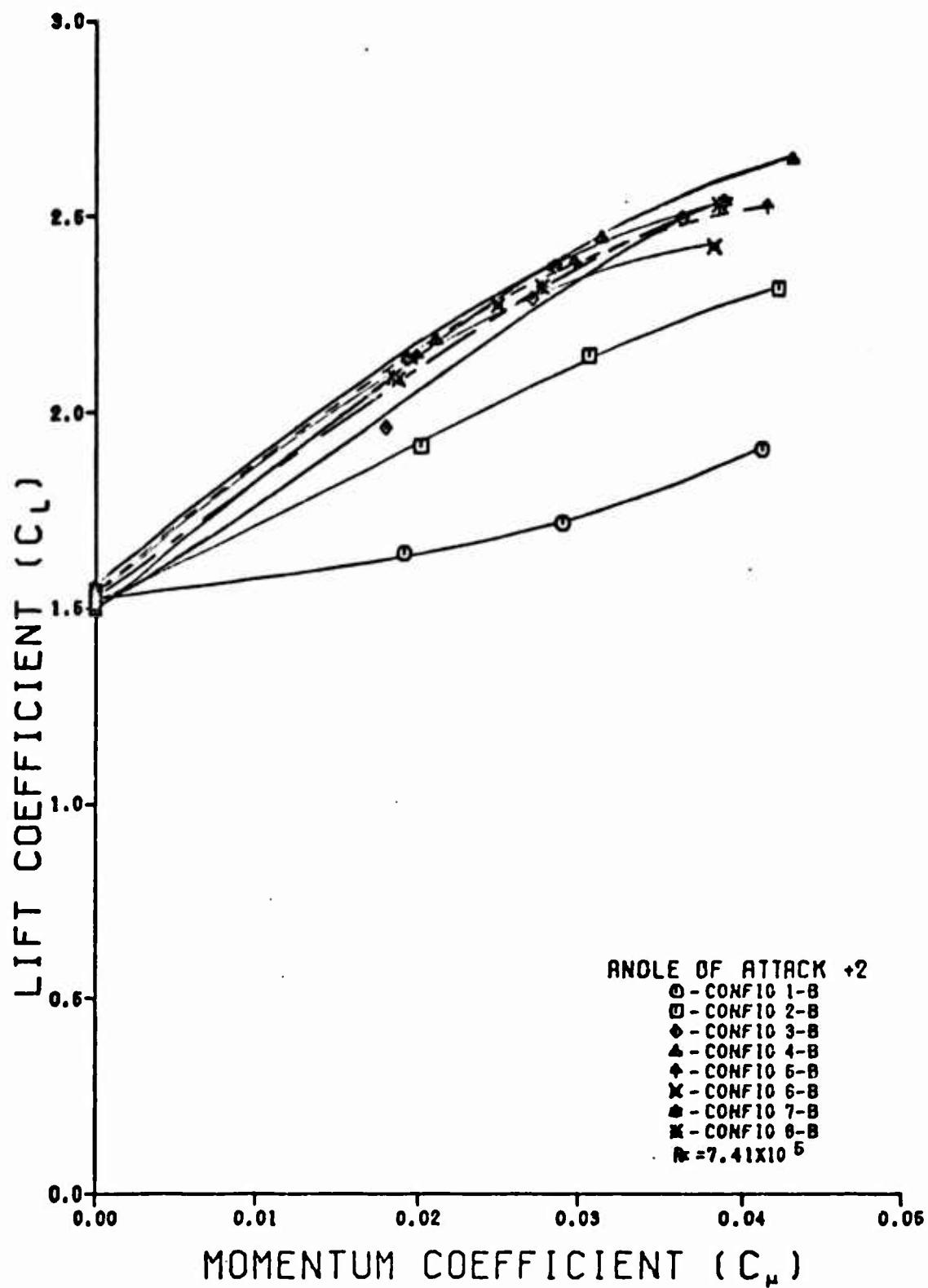


Fig. 9. The Effect of C_μ on C_l for Eight Airfoil Configurations at +2 Degrees Angle of Attack

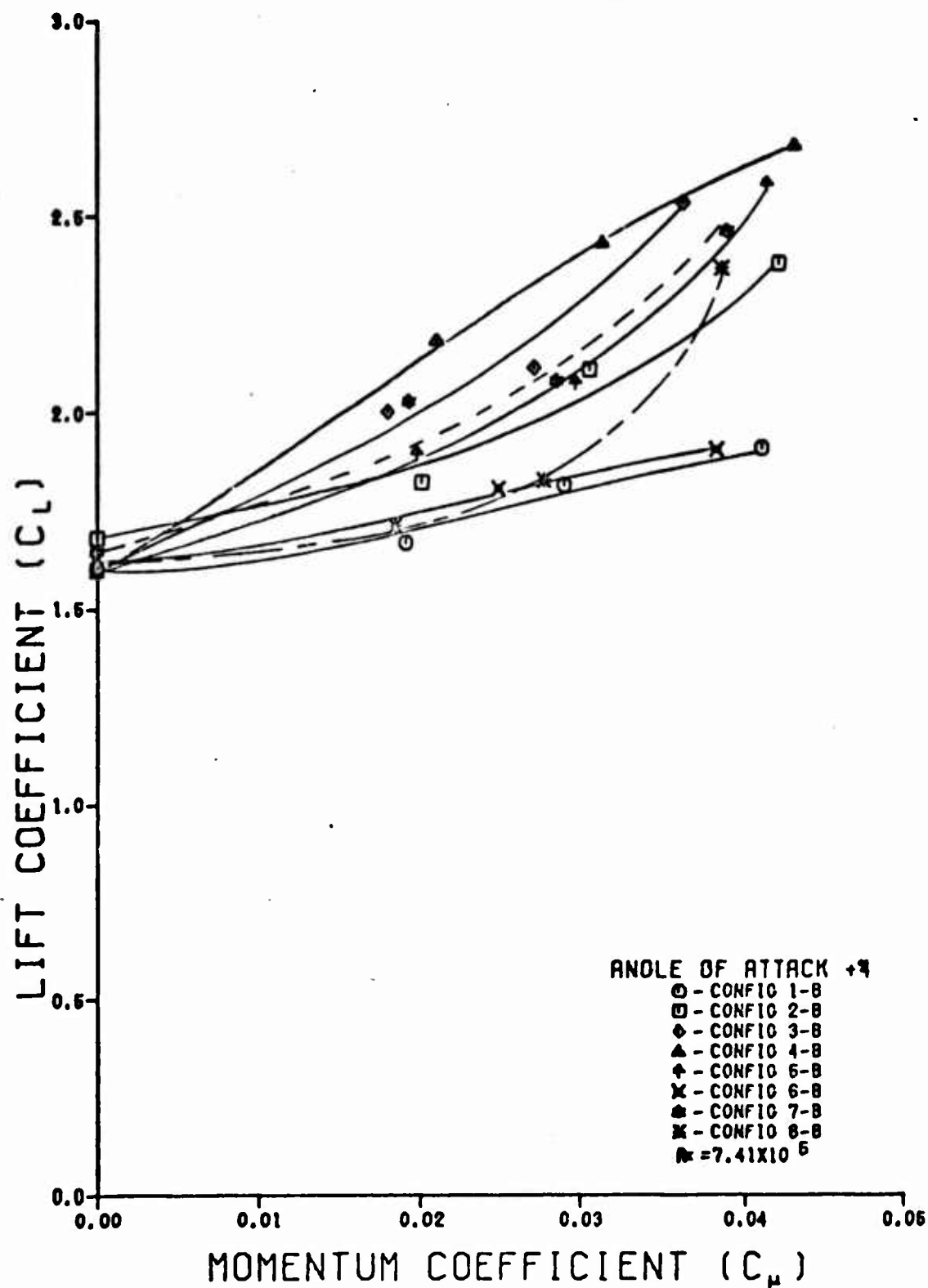


Fig. 10. The Effect of C_μ on C_l for Eight Airfoil Configurations at +4 Degrees Angle of Attack

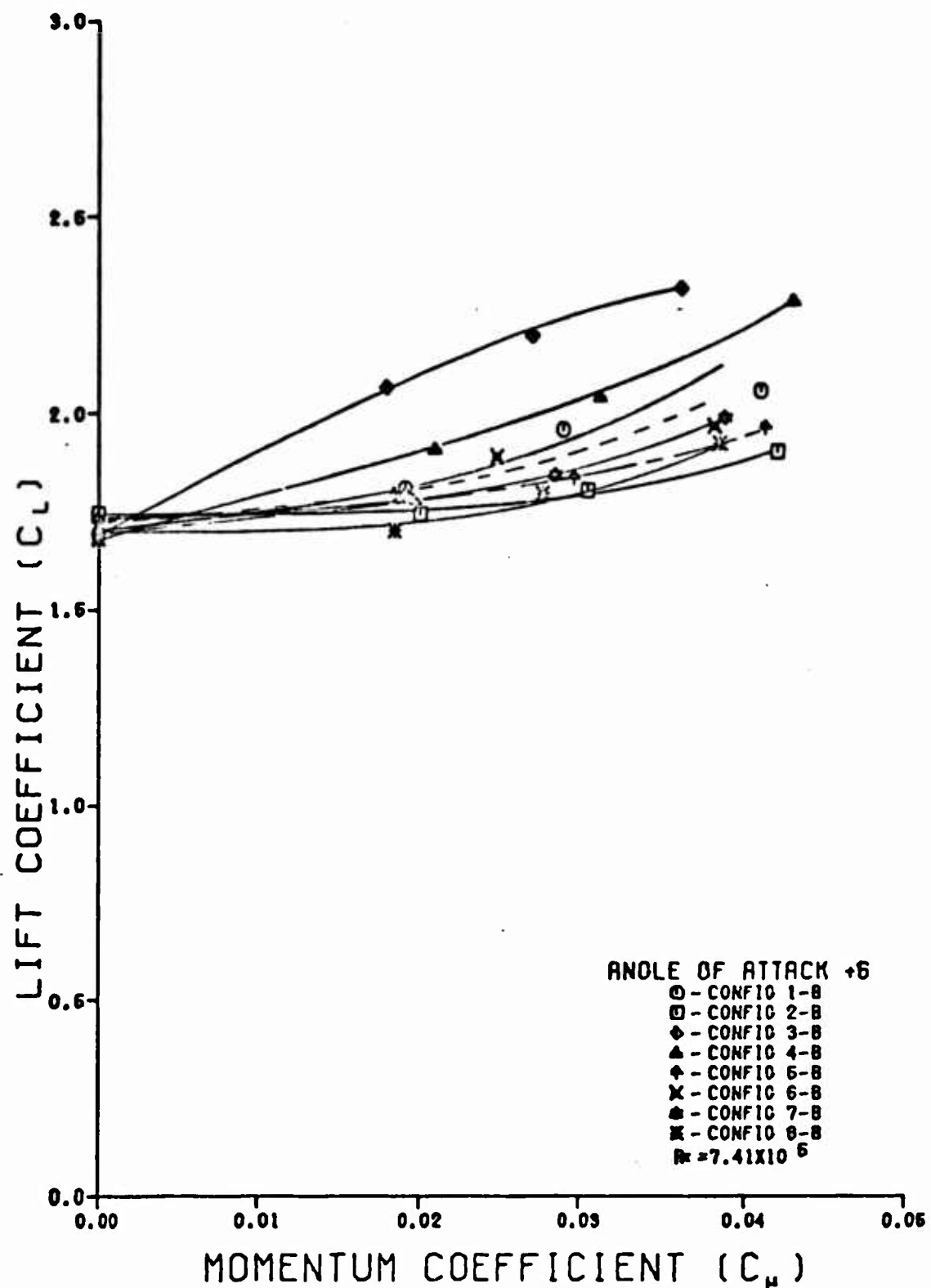


Fig. 11. The Effect of C_{μ} on C_L for Eight Airfoil Configurations at +6 Degrees Angle of Attack

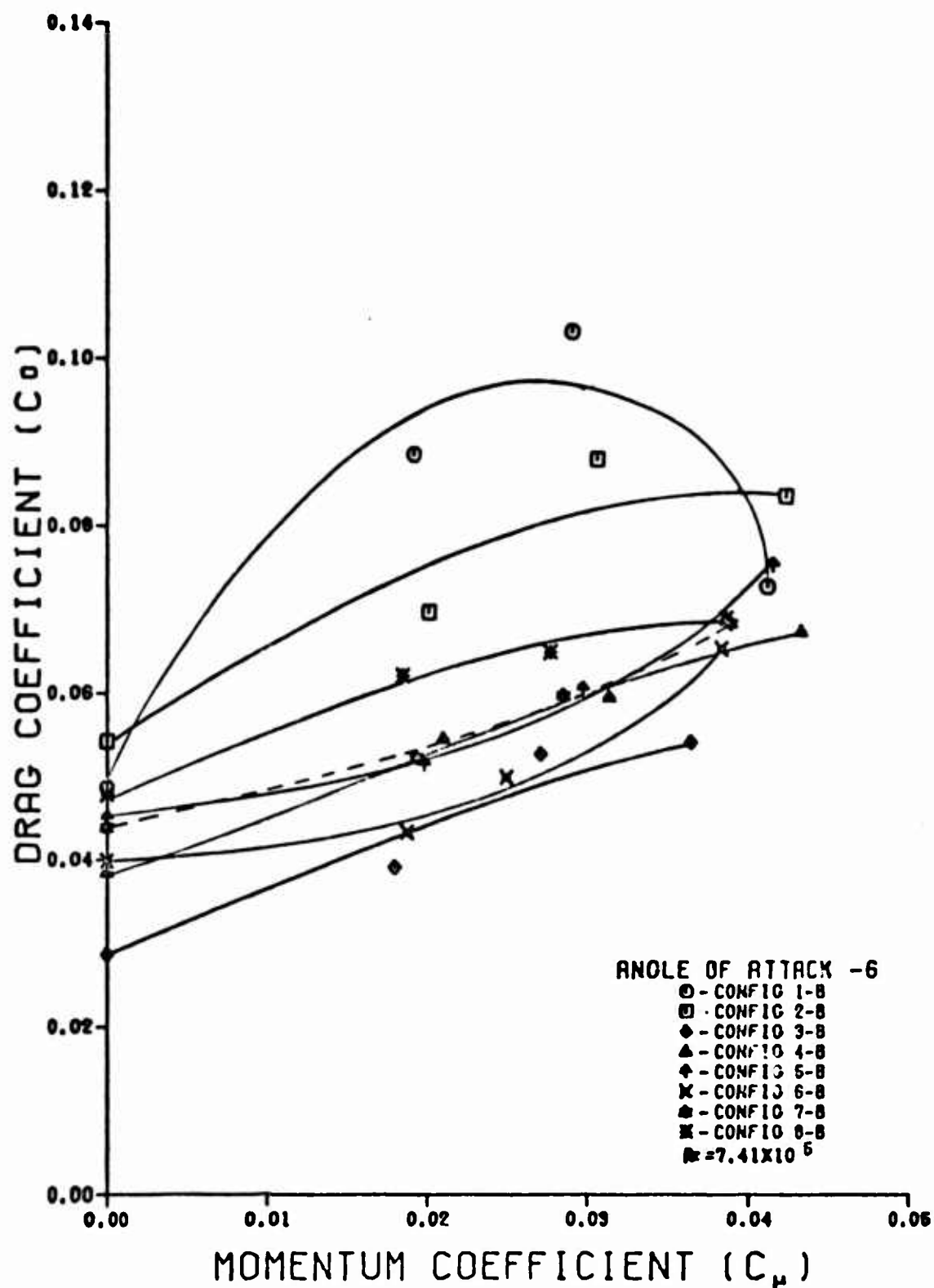


Fig. 12. The Effect of C_{μ} on C_D for Eight Airfoil Configurations at -6 Degrees Angle of Attack

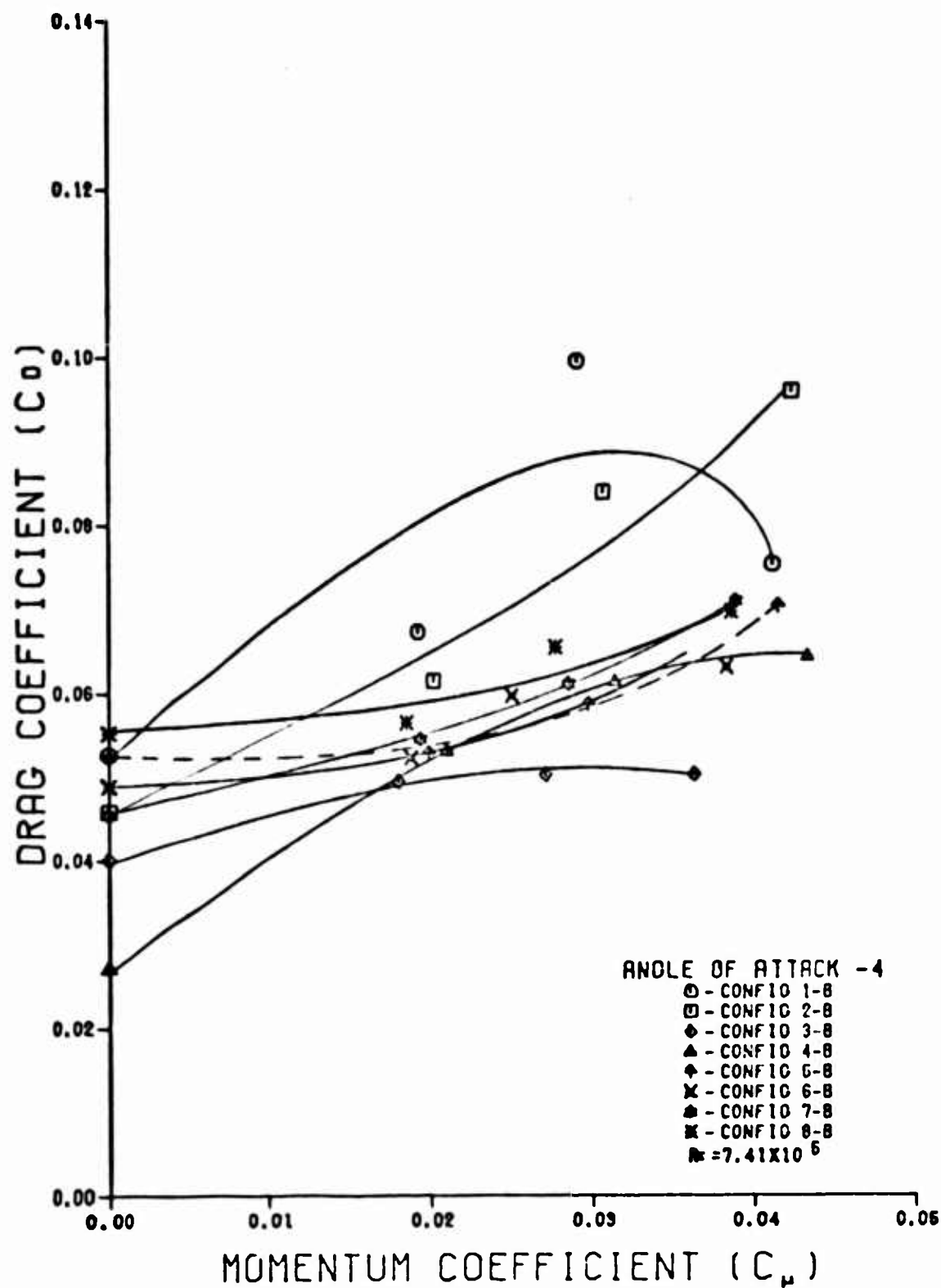


Fig. 13. The Effect of C_{μ} on C_D for Flight Airfoil Configurations at -4 Degrees Angle of Attack

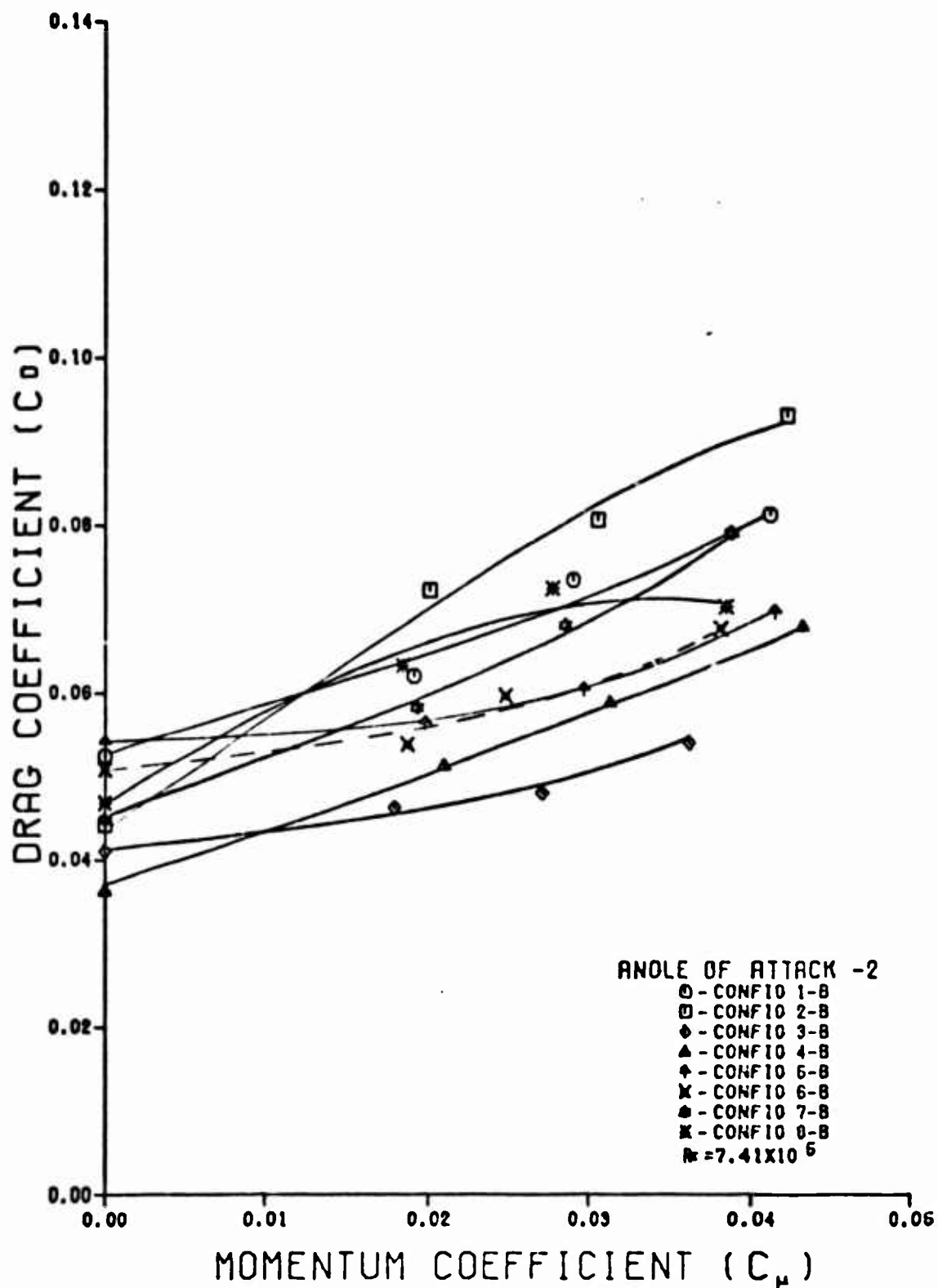


Fig. 14. The Effect of C_μ on C_{D_t} for Eight Airfoil Configurations at -2 Degrees Angle of Attack

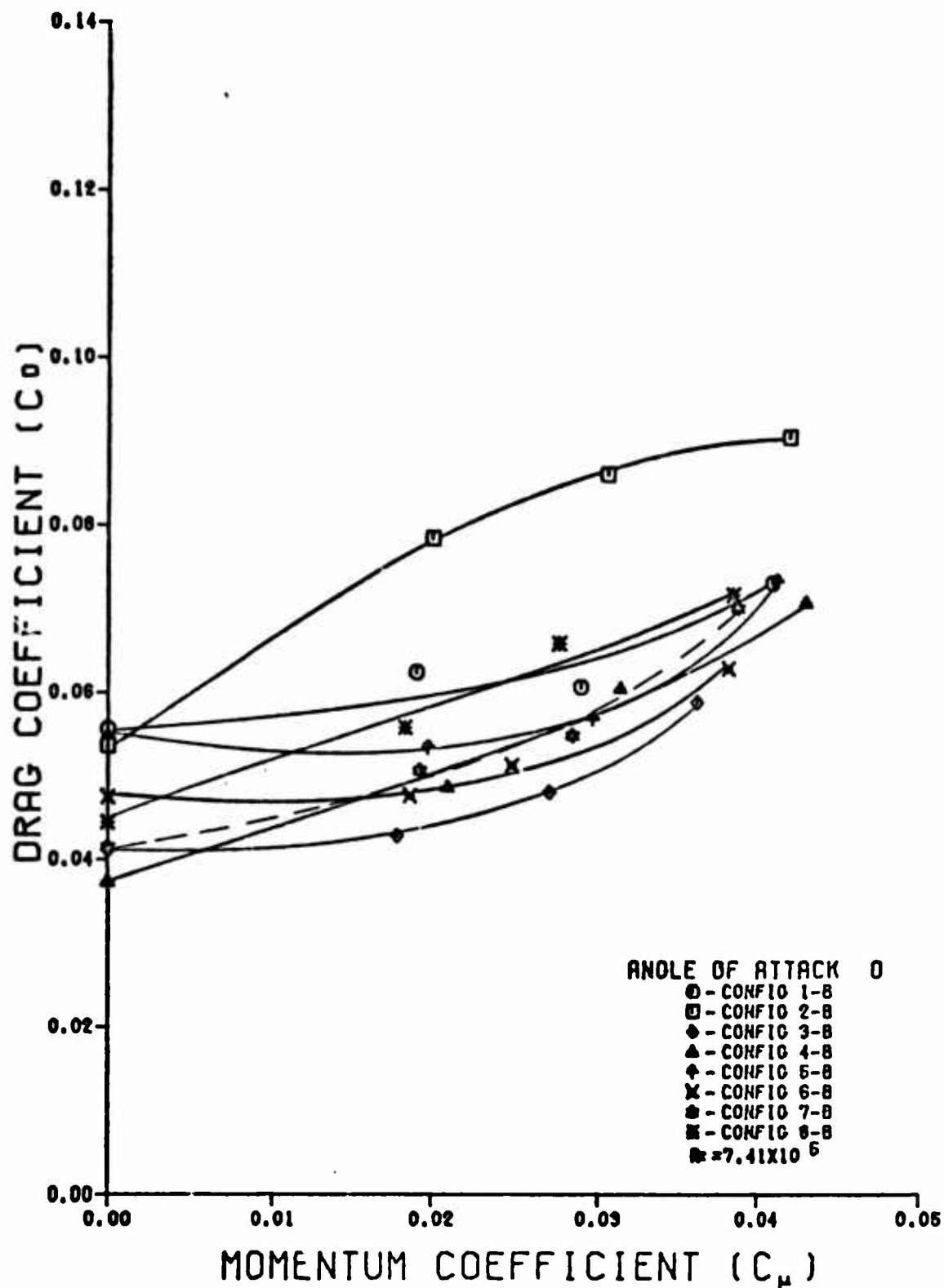


Fig. 15. The Effect of C_μ on C_{D_t} for Eight Airfoil Configurations at 0 Degrees Angle of Attack

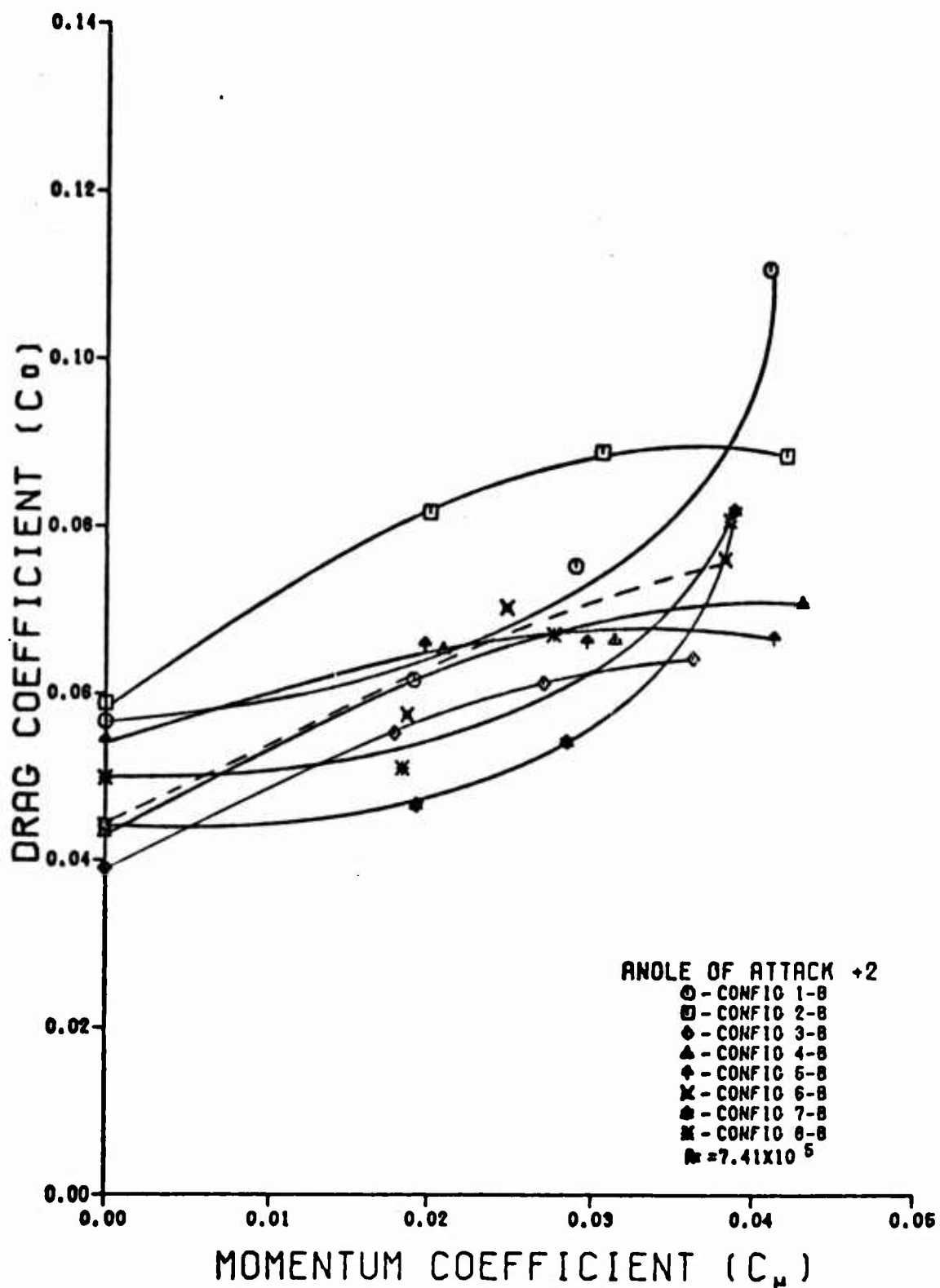


Fig. 16. The Effect of C_{μ} on C_{D+} for Eight Airfoil Configurations at +2 Degrees Angle of Attack

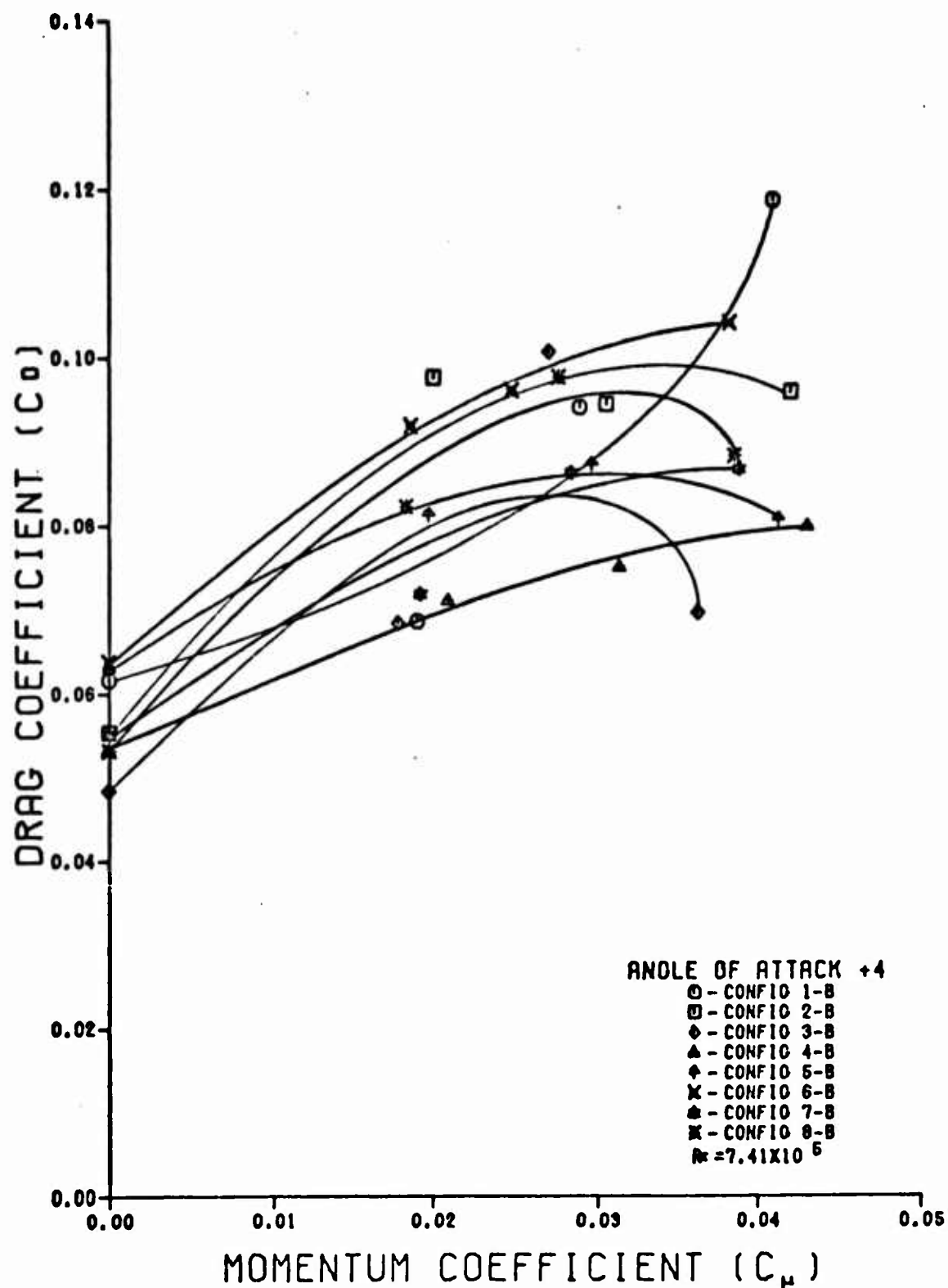


Fig. 17. The Effect of C_{μ} on C_{D_t} for Eight Airfoil Configurations at +4 Degrees Angle of Attack

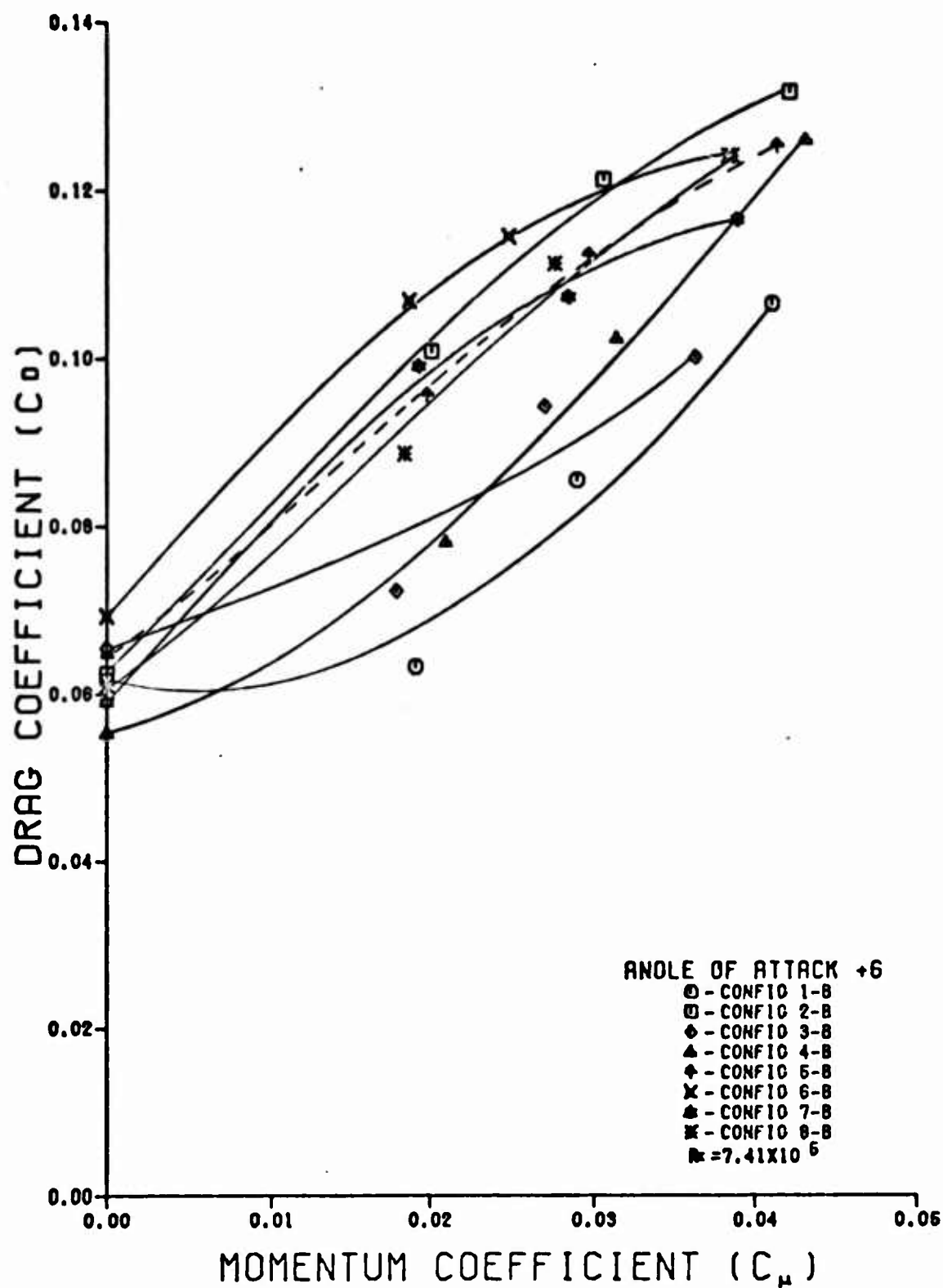


Fig. 18. The Effect of C_μ on C_{dt} for Eight Airfoil Configurations at +6 Degrees Angle of Attack

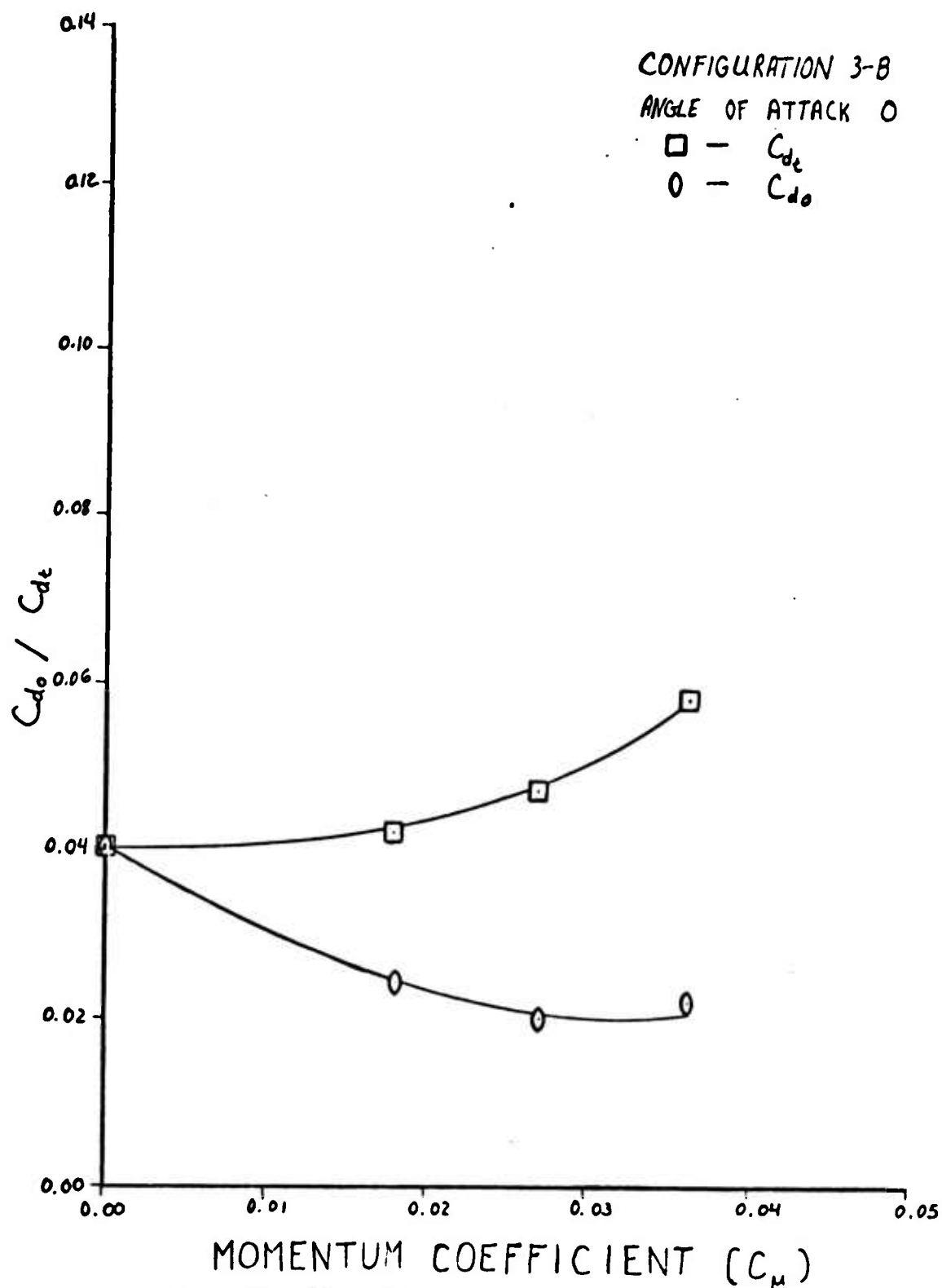


Fig. 19. The Effect of C_m on C_{do} and C_{dt} at 0 Degrees Angle of Attack

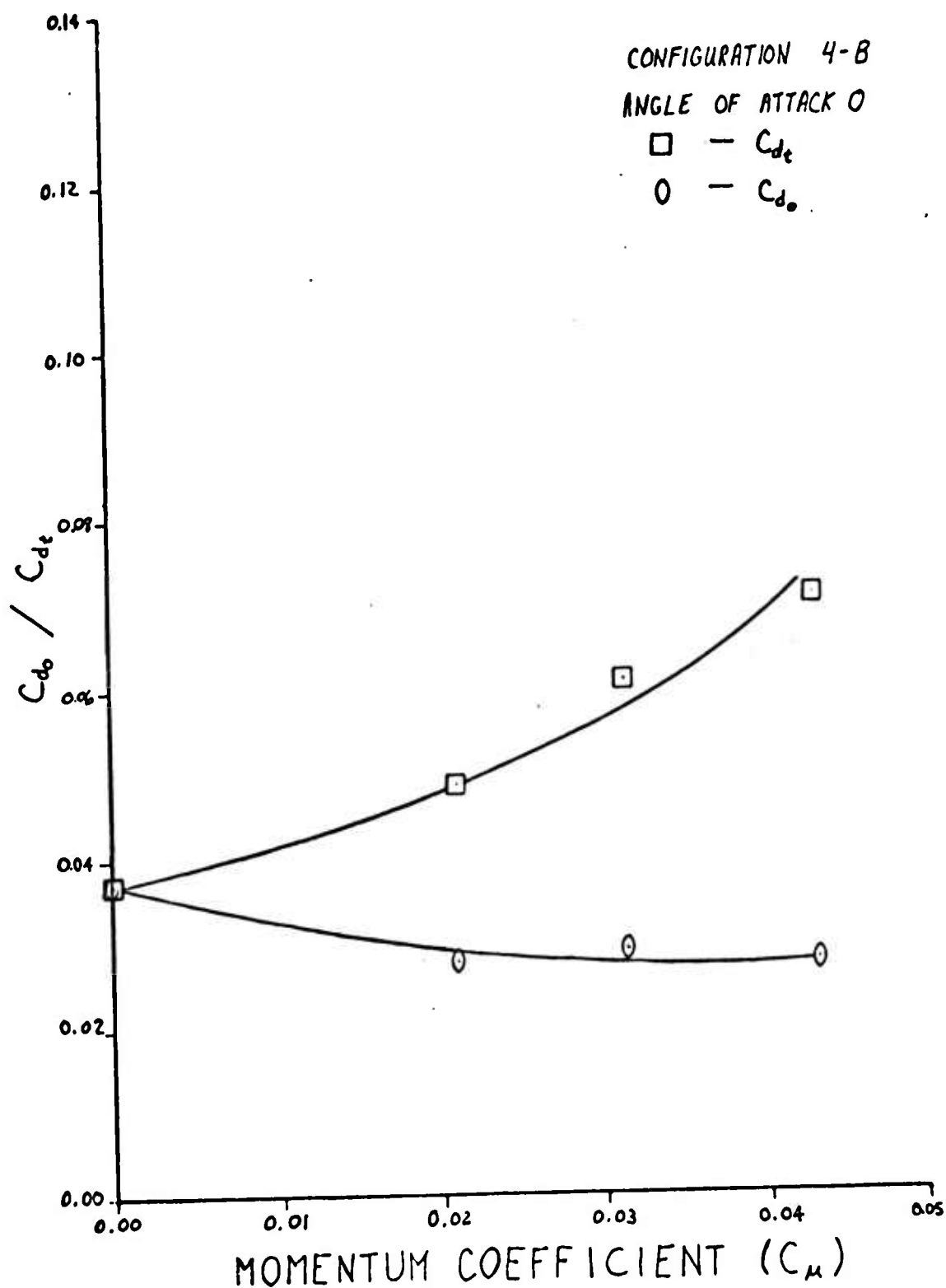


Fig. 20. The Effect of C_μ on C_{d0} and C_{dt} at 0 Degrees Angle of Attack

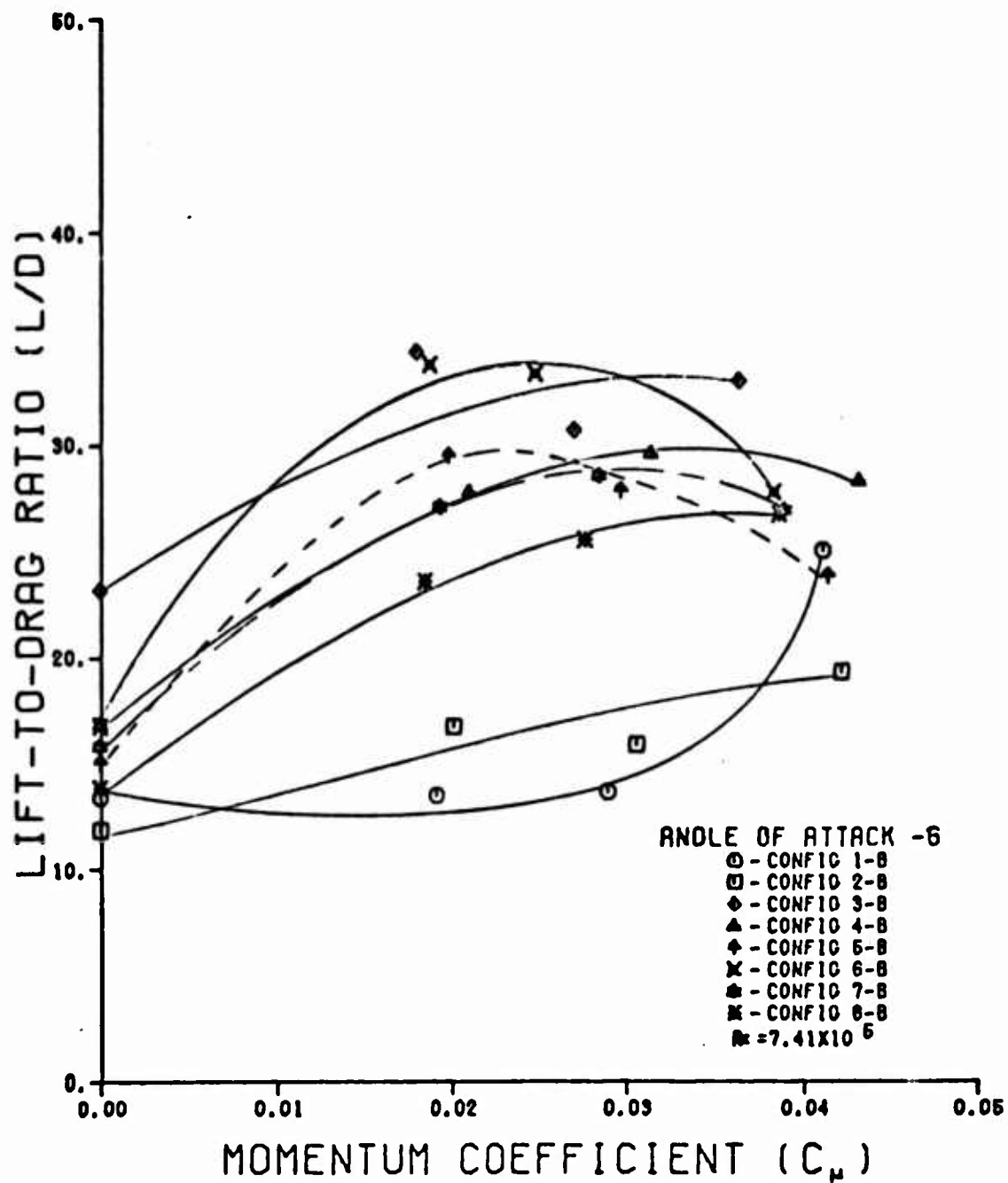


Fig. 21. The Effect of C_{μ} on l/d for Eight Airfoil Configuration at -6 Degrees Angle of Attack

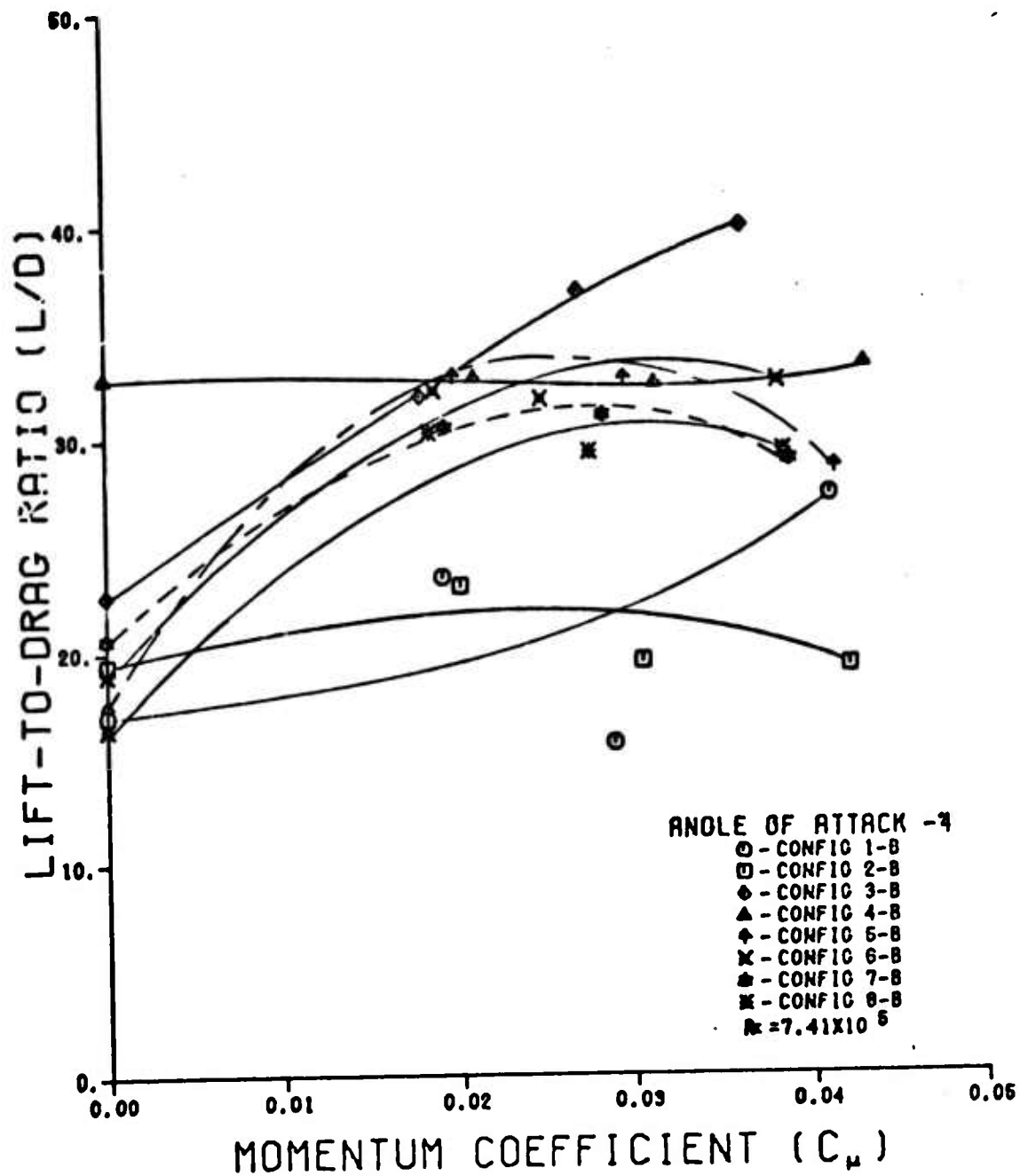


Fig. 22. The Effect of C_μ on l/d for Eight Airfoil Configurations at -4° Degrees Angle of Attack

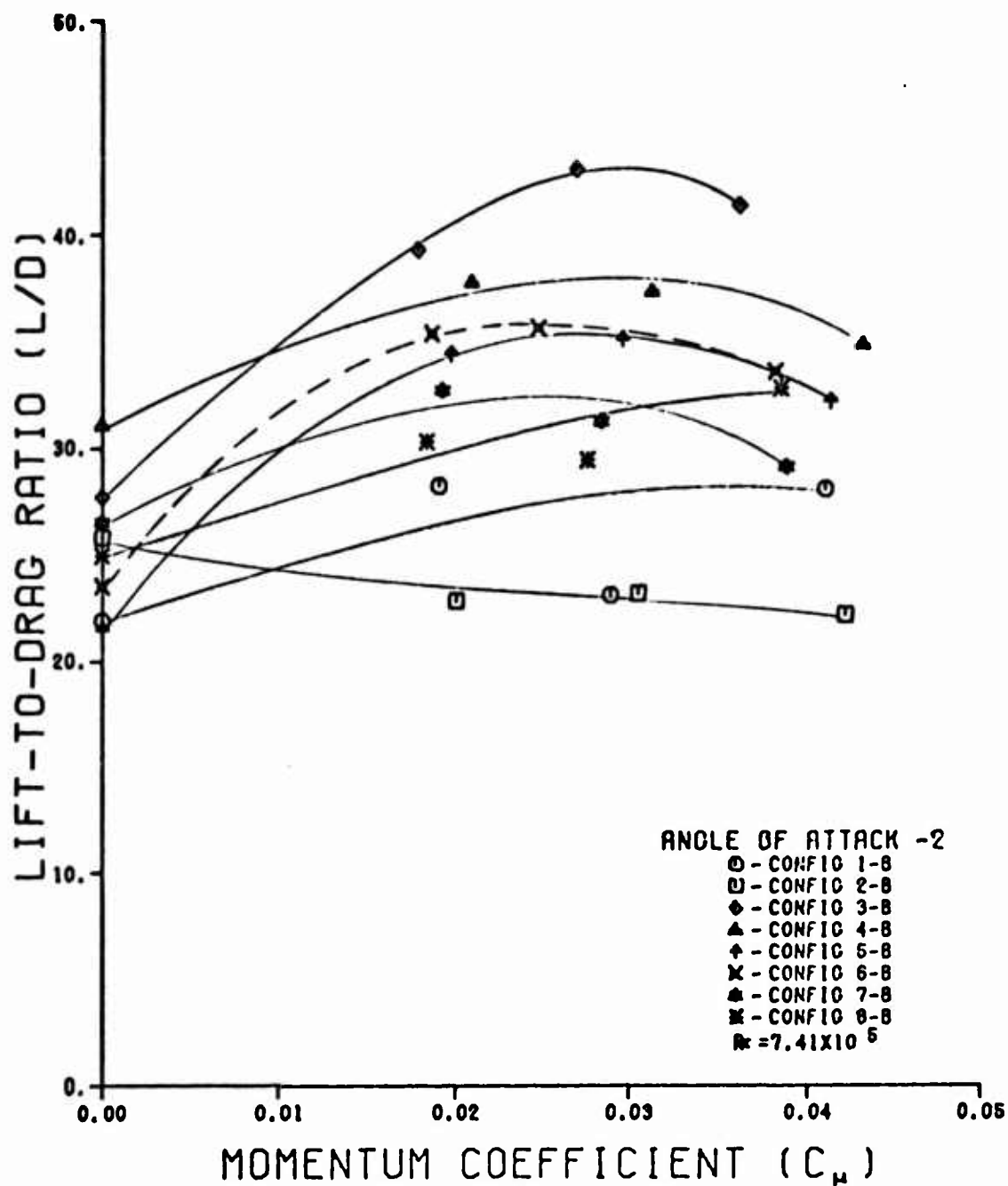


Fig. 23. The Effect of C_{μ} on l/d for Eight Airfoil Configurations at -2 Degrees Angle of Attack

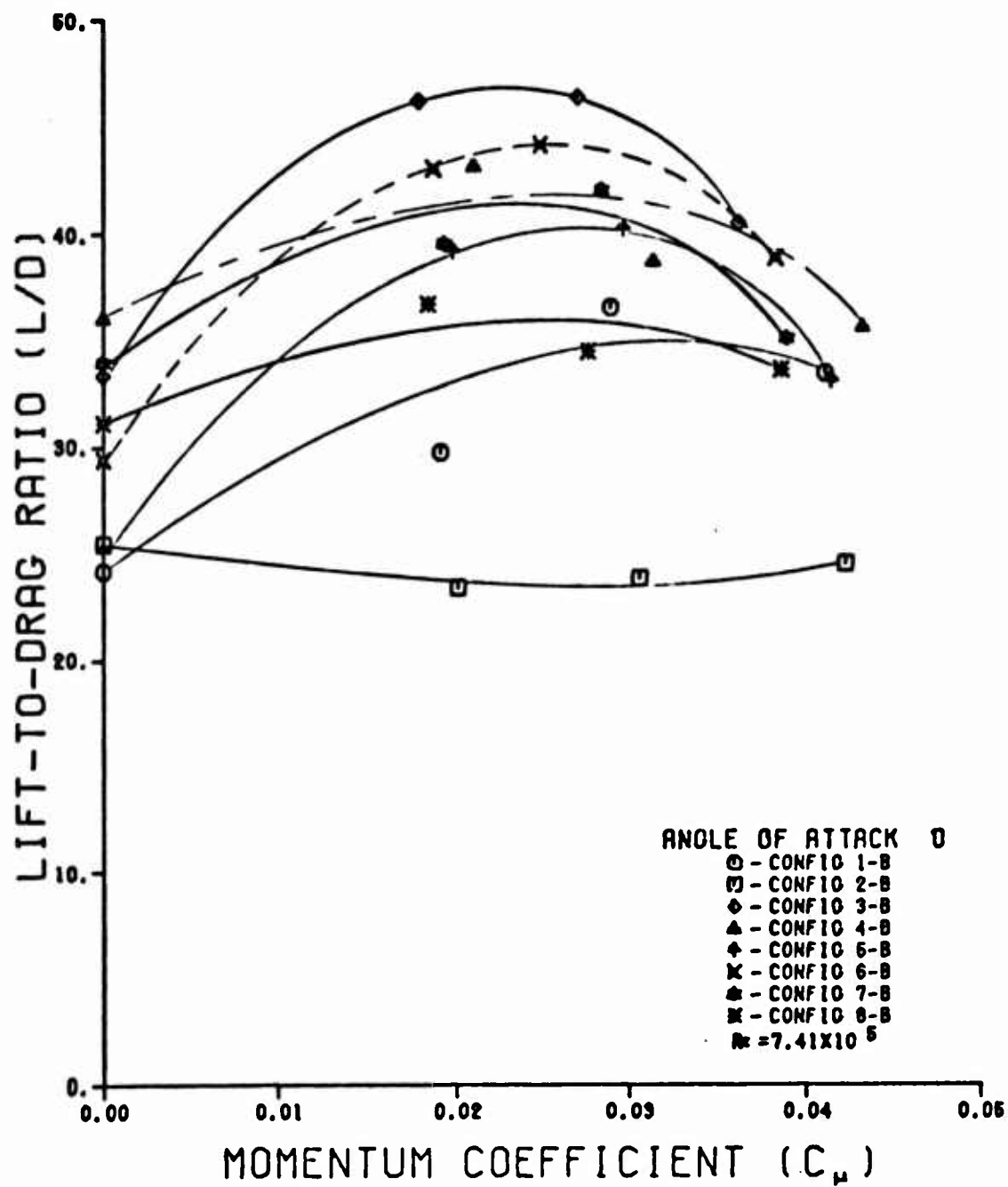


Fig. 24. The Effect of C_{μ} on L/d for Eight Airfoil Configurations at 0 Degrees Angle of Attack

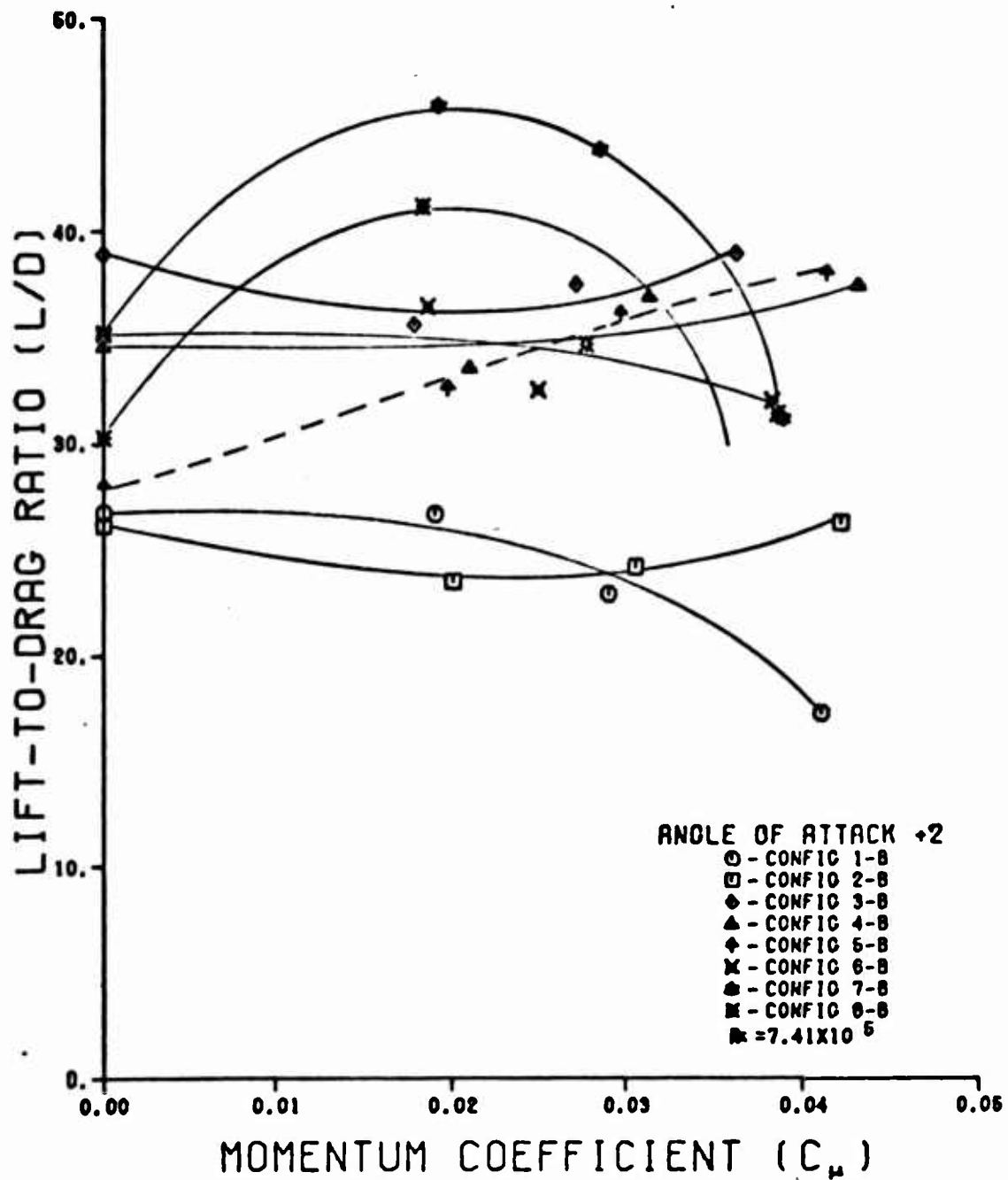


Fig. 25. The Effect of C_{μ} on l/d for Eight Airfoil Configurations at +2 Degrees Angle of Attack

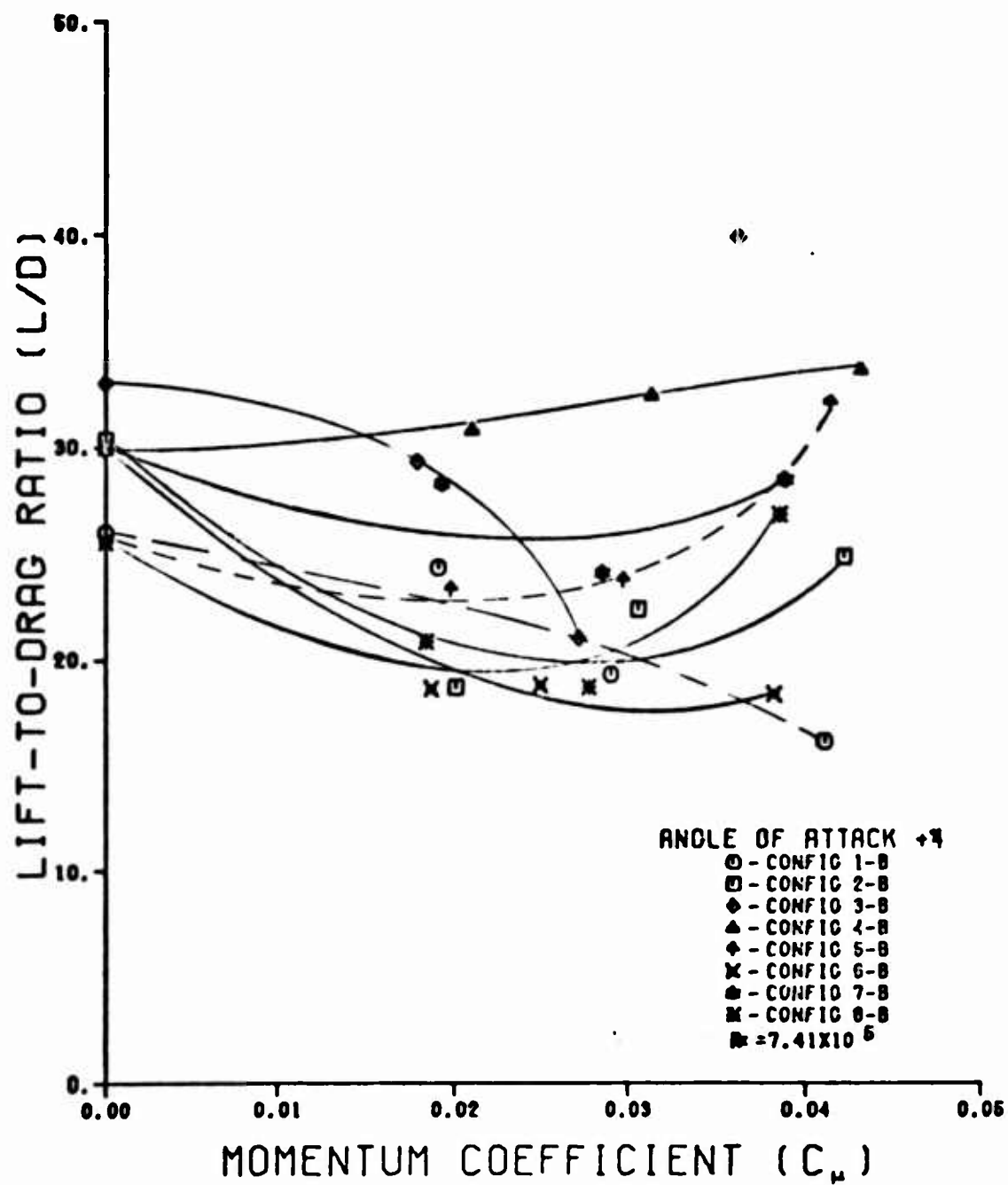


Fig.26. The Effect of C_{μ} on l/d for Eight Airfoil Configurations at 4° Degrees Angle of Attack

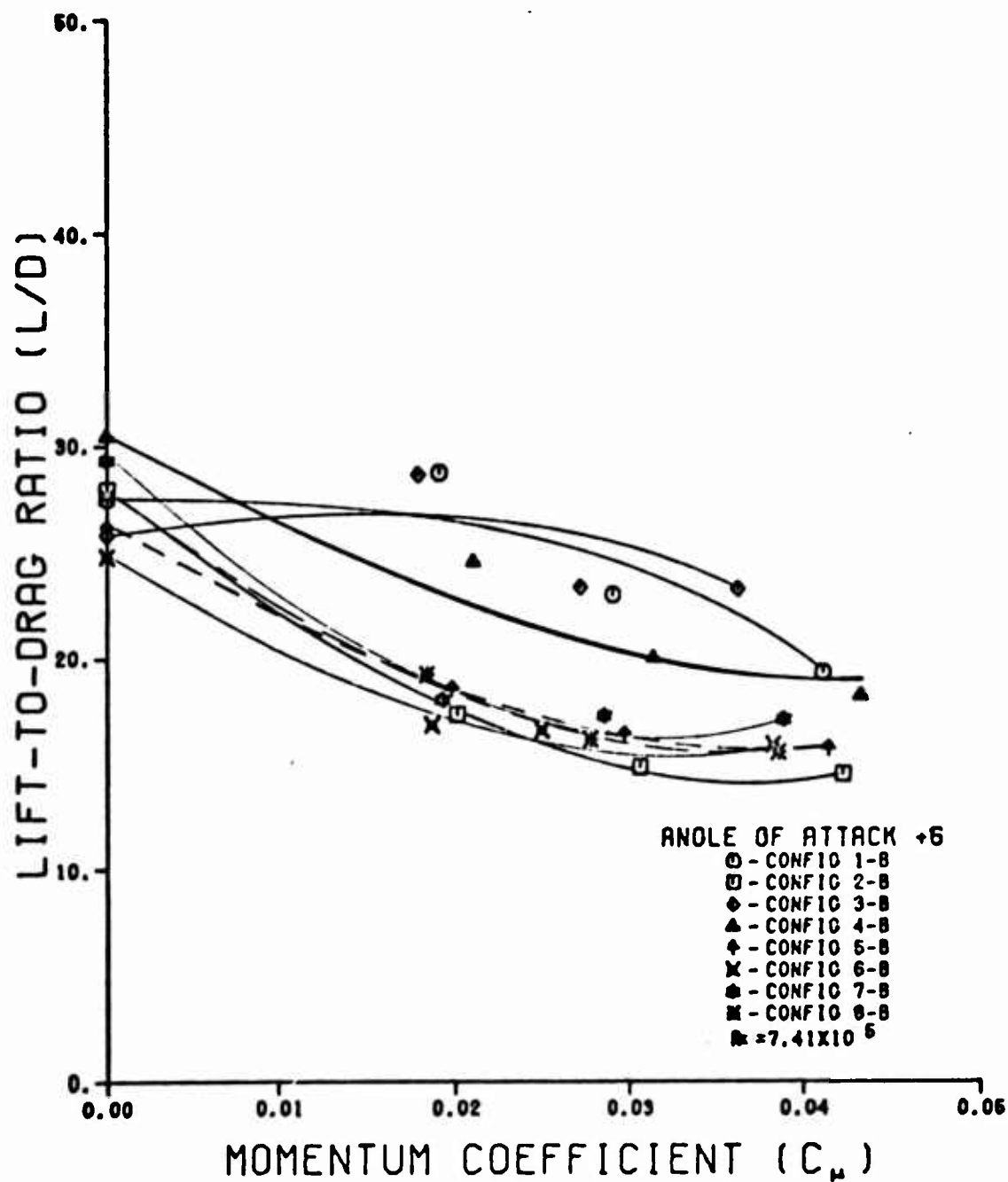


Fig. 27. The Effect of C_{μ} on l/d for Eight Airfoil Configurations at +6 Degrees Angle of Attack

Vita

Vayl Stanley Oxford was [REDACTED]

[REDACTED] He graduated from [REDACTED]
[REDACTED] in 1970, and attended the United States Military Academy,
receiving a Bachelor of Science degree and a commission in the
United States Air Force in June 1974. Following graduation, he
began study at the Air Force Institute of Technology in September
1974.

Permanent address: [REDACTED]
[REDACTED]

This thesis was typed by Mrs. Joyce Clark.